2022

AN EXPERIMENTAL STUDY TOWARDS UNDERWATER PROPULSION SYSTEM USING STRUCTURE BORNE TRAVELING WAVES

Shreyas suhas Gadekar
Michigan Technological University, sgadekar@mtu.edu

AN EXPERIMENTAL STUDY TOWARDS UNDERWATER PROPULSION SYSTEM USING STRUCTURE BORNE TRAVELING WAVES

By

Shreyas Suhas Gadekar

A THESIS

Submitted in partial fulfillment of the requirements for the degree of

MASTER OF SCIENCE

In Mechanical Engineering

MICHIGAN TECHNOLOGICAL UNIVERSITY

2022

This thesis has been approved in partial fulfillment of the requirements for the Degree of MASTER OF SCIENCE in Mechanical Engineering.

Department of Mechanical Engineering - Engineering Mechanics

Thesis Advisor:	*Dr. Sriram Malladi*
Committee Member:	*Dr. Kazuya Tajiri*
Committee Member:	*Dr. Susanta Ghosh*
Department Chair:	*Dr. William W. Predebon*

Table of Contents

List of Figures

List of Tables

Acknowledgements

Finally, it’s time for me to acknowledge and appreciate everyone who were always there to help and support me in this wonderful journey. First and most important, I would like to thank my supportive advisor Dr. Sriram Malladi. I am so fortunate to have you as my guide for this research project. I am grateful to you for providing me with such an opportunity to enhance my skills and set me in a right direction. When I first met you, I was not sure about the research I wanted to do, but you patiently let me try many topics to check where I can be a better fir. Many times, I got distracted and lost my motivation to work as I was not getting any results, but you were always easygoing with me and supported me in my difficult time. I can’t thank you enough for mentoring me. I also want to thank my committee members Dr. Tajiri and Dr. Ghosh for their guidance in this process and giving me instructions for improving my thesis.

My colleagues have helped me so much in this journey. A special thanks to Hrishikesh and Shantanu for helping me with the setup and working with me to shoot the videos for image processing. I also want to thank my friends Ajinkya and Rahul for supporting me morally when I was feeling down. And now there are two people for whom just a thank you is not enough. My dad Mr. Suhas Gadekar and my mother Mrs. Sayali Gadekar dedicated their whole life for my ambitions and growth. They always pushed me to do more in my life and whatever success I have is because of them. I am really blessed to have such parents.

Abstract

The method of generating steady-state structure-borne traveling waves underwater in an infinite media creates abundant opportunities in the field of propulsive applications, and they are gaining attention from several researchers. This experimental study provides a framework for harnessing traveling waves in a 1D beam immersed under quiescent water using two force input methods and providing a motion to an object floating on the surface of the water.

In this study, underwater traveling waves are tailored using structural vibrations at five different frequencies in the range of 10Hz to 300Hz. The resulting fluid motion provides a propulsive thrust that moves a 3D-printed bob floating on the surface of the water. The undulatory motion of the floating bob is determined using an image processing approach. In this approach, videos are recorded for image processing to determine the effects of each traveling wave frequency on the object's motion. Through image processing, observations are drawn regarding the velocity and the distance traveled by the bob for each SBTW frequency.

As this is developing research, there is a limited understanding to the relationship between the amplitude of force input, the traveling wave frequency, and the velocity attained by the object. So, with the help of image processing, a general observation about the effects of varied force input on the motion of the object at each frequency is drawn.

Chapter 1

Introduction

1.1 Introduction

The recent increase in the demand for underwater vehicles for ocean exploration opens doors to numerous possibilities in the technological advances for efficient propulsion systems. Researchers are constantly striving to mimic the swimming pattern of various marine organisms to enhance the maneuverability and efficiency of autonomous underwater vehicles [1]. The propulsion system for such vehicles usually uses many rotating parts and actuators which limits the efficiency of the overall system due to high maintenance [2]. So, the objective of this research is to develop a foundation for generating underwater propulsive forces using minimum rotating parts and actuators.

The expanding need for such type of propulsion mechanism directed the attention of researchers towards generating the undulatory motions in finite structure which opened numerous applications which were not possible before [3]. This experimental study greatly deals with generating underwater propulsive forces through harnessing study state structure-borne traveling waves in 1D beams and proving that it could be used for advanced underwater propulsive applications.

Researchers are constantly studying the different types of waves that are provided by nature and what applications they possess. There are many types of waves available in nature, but this research specifically revolves around understanding the behavior and

development of underwater steady-state structure-borne traveling waves through finite media.

Therefore, the following chapters of this work would discuss the experimental generation of structural traveling waves in a beam immersed underwater and create a framework that would help to design the further applications it. The next step would be to provide the occurrence of such waves in nature and the studies performed to understand their behavior and different types of propulsive systems used in underwater vehicles.

1.2 Research Objective

This is an experimental study, so the first objective of this research is to construct a setup for achieving steady state traveling waves underwater in a 1D aluminum beam and testing its effects on the water surface. The second step after achieving this would be to use two force excitation methods for the generation of traveling waves.

This method has been successfully proved and implemented by many researchers in their previous works using piezoelectric crystals [4-7]. But, in this study instead of piezoelectric actuators, shakers are used as a force excitation method. Underwater wave generation requires high force input with a low-frequency range which could be easily delivered by shakers. Piezoelectric actuators are useful for high-frequency range applications.

Moving further the third objective would be to immerse the setup underwater to tailor steady-state traveling waves at multiple frequencies in a defined direction with controlled

amplitude which would create water current along the surface of the aluminum beam. The generated thrust in water should be able to carry an object with the flow from one end to another end.

After the successful thrust generation and object movement, the last research objective is to perform image processing to investigate the velocity of an object moving on the surface of the water to the frequency. This would give us a clear picture of the relationship between the velocities or the thrust generation of an object versus the frequency used to generate the traveling wave.

1.3 Motivation

Our surroundings and the universe have always been the source of inspiration for numerous research and inventions. This research is derived from the occurrence of mechanical waves existing in nature and how bio-organisms use them for different applications. Before going forward, it is necessary to understand what mechanical waves are and what their types are. So, the mechanical waves can be classified into traveling waves, standing waves, and hybrid waves [6]. The generation of these waves depends on the type of force input, the boundary conditions, and the structure where waves are generated. Typical steady state traveling waves propagate continuously from one end of the structure to other without making reflections on boundaries in a finite medium while carrying energy through the structure [8, 9]. On the other hand, standing waves are stationary waves oscillating concerning time keeping the peak amplitude profile constant

at any point in space and time. The third type of wave is a hybrid wave which is a combined response of traveling and standing waves [4].

A most common place where a traveling wave exists is in the undulatory motion of underwater micro-organisms. Researchers have been interested in bio-organisms with such swimming motion since 1951 [10, 11]. According to the previous studies conducted, Flagella, a type of bacteria with a hair-like structure, has a head and tail as its body creates a translational thrust by generating a wave that travels along its body from head to tail [12]. The motion's direction of flagella swimming underwater is determined by the ratio of tangential force by the normal viscous force.

Besides the study on micro-organisms for traveling waves, researchers also showed interest in macro aquatic animals for their swimming methods. They discovered that most aquatic organisms either travel through paddling mechanisms, using water jet-powered mechanisms, or wave propagation. They also studied that using propellers for underwater vehicles is not an effective method of propulsion as it is just 40% efficient [13]. To solve this issue the best way is to use smart materials such as Ionic polymeric metal composites, shape memory alloy, and piezoelectric crystals.

Since then, researchers have tried to replicate the propulsion system experimentally and numerically such as jellyfish-inspired underwater vehicles using ionic polymer-metal composite actuators [14]. They also worked on developing monolith ionic-polymer metal composite (IPMC) fins for stable maneuverability of the underwater vehicles [15, 16] where smart materials are used to actuate the fins of aquatic robots mimicking the

swimming characteristics of a fish. In most cases, the fin is integrated with the robot using multiple attachments to create multiple small oscillations resulting in a whole traveling wave that could induce propulsive forces in the robot.

Another area where we could observe naturally occurring traveling waves is any mammalian's ear. The pressure waves created by a source when reaches the ears actuates the eardrum and the wave is transmitted to the cochlea where the sensory unit of the ear lies [17]. The sound pressure waves then propagate to the basilar membrane as a traveling wave. Researchers have presented that with this phenomenon the multiple frequencies traveling waves interacting with the cochlear mechanism through cochlear fluid could be used to construct a system with variable stiffness. Many bio-inspired mechanisms use different waves for different applications, such as the ocean, birds, and reptiles. But most research focus on mimicking the motion pattern rather than generating the structural wave.

Few of the advanced studies working towards generating structural traveling waves have found out that, a wave-generated in finite medium tends to reflect at the boundaries because of changes in impedances resulting in a standing wave [18]. Researchers were able to classify the role of impedance in wave propagation into two field i.e., structure-borne traveling wave generation and vibration suppression [19]. Piezoelectric actuators were used for vibration suppression studies by dampening the wave propagation using a shunt electrical circuit which would control the structural vibrations [20]. In the case of the generation of traveling waves using piezoelectric, partial vibration suppression was necessary which would dampen the reflections caused due to impedance change at

boundaries. This concept was proved by researchers using numerical and experimental methods [3-5,17,18].

In this section, a variety of applications and research were discussed associated with naturally occurring and generation of traveling waves. With this review, it could be understood that the generation of traveling waves has a wide range of applications and it has got a very good potential to work as a medium to transport material through its propulsive forces. In the next section, the previous work performed to generate structure-borne traveling waves would be discussed.

1.4 Previous work done on generation of traveling waves

As mentions in the earlier section, mechanical waves could be classified according to the transfer of energy i.e., traveling waves and standing waves. The wave which carries energy along its direction to a distance is known as a traveling wave and the wave where the energy is constrained to a specific location is known as a standing wave. From the previous research [4, 21], it is known that if a single force is applied to a structure it tends to vibrate and generate waves. These waves are then reflected due to impedance changes.

Consider a beam with clamped – clamped boundary conditions, as a single point force is applied to this case; a wave is generated and then reflected from the other end acting as an incident wave. Both waves have the same magnitude and the combination of those forms a standing wave with an equation of $w(x, t) = A\sin(wt - kg) \pm B\sin(wt + kx)$ where amplitude A equals amplitude B. But when the beam is excited using two single-point force inputs using the same frequency with a phase offset, then the part of a

reflected wave is neglected because A ≠ B. The combination of these waves results in a hybrid wave were components of the traveling wave, as well as a standing wave, are present. The quality of the traveling wave is dependent on two factors i.e., excitation frequency and phase offset. Figure 1.1 has shown the plots for a pure traveling wave, standing wave, and hybrid waves

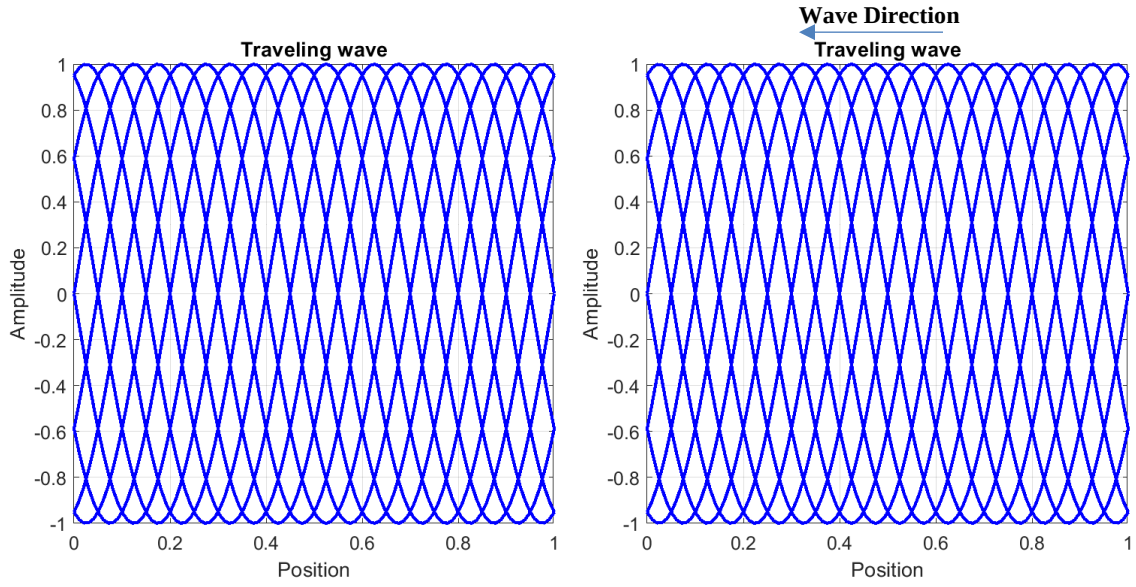

a) A ≠ 0 B = 0 **b)** A = 0 B ≠ 0

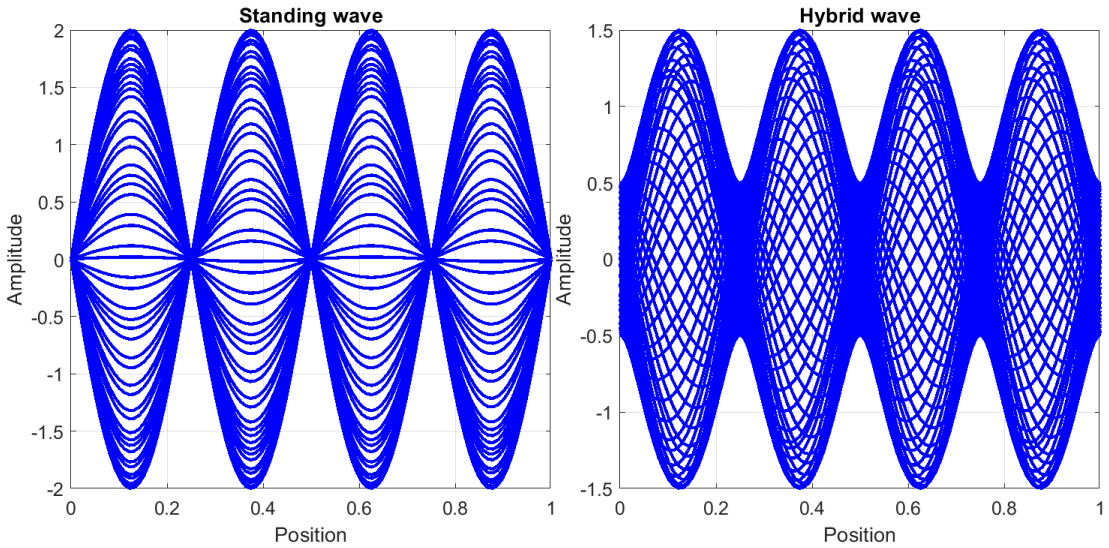

c) $A = B \neq 0$ **d)** $A \neq B \neq 0$

Figure 1.1: *Description for different wave formations in a finite media*

The above theory is an important foundation for this experimental research to successfully generated underwater traveling waves. So, to tailor a traveling wave, a structure needs to be excited in a way that would influence its dynamic response. This work utilizes modal shakers as the source for excitation as they have higher forcing signals and are more efficient for low-frequency ranges than piezoelectric elements.

Pure traveling waves are extremely difficult to generate in a finite structure experimentally. Only, in theory, pure traveling waves are observed in an infinite structure without boundaries. As soon as boundary condition comes into play in experimentation, waves tend to get reflected at boundaries resulting in standing waves. Therefore, it is impractical to generate pure traveling waves in a finite structure. But in recent studies, there have been successful attempts in generating traveling waves in strings, beams, rods, and 2D surfaces [3, 6].

Dr. Malladi in [22] has developed a numerical modal to generate traveling waves in a 1D beam with different boundary conditions i.e., clamped – clamped, free – free, and clamped – free to study the behavior of traveling waves in such cases. This model was experimentally validated on a brass beam using two piezoelectric elements as force inputs. This experimental study of tailoring high-quality traveling waves was also conducted on thin 2D plates with multiple piezoelectric actuators [23]. By generating TWs in a 2D plate, it was found out that the location of actuators should be either

symmetric or anti-symmetric about the y-axis and should be simultaneously excited else asymmetric forces would be induced in the structure.

1.4.1 Cost function for wave identification

According to their behavior mechanical waves are classified into standing waves, traveling waves, and hybrid waves. Pure standing waves are having nodal points where the deflection of a structure is zero while a pure traveling wave does not have nodal points and the wave propagates with a constant amplitude concerning time. Then there is a hybrid wave which is the combined response of traveling wave and standing wave where the non-varying amplitude propagates and oscillate transversely simultaneously. It is very difficult to classify a wave into these categories as the dominance of traveling wave or standing wave component is unknown. So, the quality of traveling waves should be quantified as it is more dependable than mere observations. This research uses a cost function to quantify the behavior of a wave using the wave envelops approach.

Waves envelop is a tool to observe the difference between different waves and their behavior. A plot that shows an area/displacement swept by a wave concerning time is known as a wave envelope. If a sharp nodal point is displayed in a wave envelope with no displacement, then it is a pure standing wave and if the displacement is constant along the length of the structure then the wave envelops shows traveling wave. But in the case of hybrid waves, the amplitude tends to vary along the length with no clear nodal point.

To identify the behavior of different waves, a hybrid wave is considered. This plot contains top and bottom curves representing the time data of the wave. From the wave

envelop the maximum values and minimum values of displacement are known and represented as Ymax and Ymin respectively. In the case of the pure standing wave, Ymin = 0, and Ymin is equal to Ymax in the case of pure traveling waves. In the case of hybrid waves the Ymax ≠ Ymin ≠ 0. From this, a cost function is derived to quantify the characteristics of a wave.

$$\mathrm{CF} = \frac{Y_{\max} - Y_{min}}{Y_{\max} + Y_{min}}$$

The values of the cost function for pure traveling and standing are 1 and 0 respectively. If the value of the cost function is 0.1 then it is considered a hybrid wave with 90% of traveling wave components and 10% of standing wave components. So, to have a high-quality traveling wave the cost function should be as close to 0 as possible. The only drawback of this method is that it involves a lot of spatial point data to plot a wave envelop of a whole structure and to get an accurate cost function.

1.5 Thesis Outline

The experimental study presented in this thesis is divided into four major chapters starting with the introduction of structure-borne traveling waves. The 1st chapter contains an introduction and literature survey for the generation of traveling waves in different materials and their prospective underwater propulsive forces. The literature survey provides a brief idea about the characteristics of different waves and how to identify them using the cost function.

In chapter 2, the previous work to generate traveling waves is used to build a test setup with two force input methods where two modal shakers are pinned at the ends of a thin aluminum beam. A scanning laser vibrometer is assembled integrating polytec's single point laser vibrometer with a polytec's scanning unit. The aluminum beam was immersed under quiescent water to acquire mode shapes and natural frequencies. An experimental modal test is performed to plot FRF's using the scanning laser vibrometer by exciting modal shakers alternatively for 31 points. The mode shapes are acquired through experimental and numerical methods and they were validated using a modal assurance chart.

The whole chapter 3 is focused on generating underwater structure-borne traveling waves in a 1D aluminum beam using the FRF data gathered from the modal testing. A numerical model is created using the modal testing data to predict prospective traveling wave frequency regions. The frequency between two consecutive natural frequencies from prospective regions is selected to plot a wave envelope of structure borne travelling waves (SBTW). The wave envelop is then validated using a cost function to achieve a good quality SBTW. These frequencies are then used in experimental testing to excite both modal shakers using a sinusoidal signal with a phase offset simultaneously to obtain high-quality underwater SBTW. The beam is then scanned for velocity measurements to plot a wave envelop of SBTW validating it with simulations.

In chapter 4, a 3D printed object is used to show the propulsive characteristics of SBTWs. While a traveling wave is generated in the beam, an undulatory wave-like motion is observed over the surface of water flowing in the direction of the traveling

wave. The object is placed over the surface of the water and its motion is tracked using a Zed2 camera. Using the tools of image processing and blob analysis, the instantaneous speed and the distance traveled by the object are evaluated. The evaluated results are then observed for some relationship between the speeds of an object to the frequency used to excite modal shakers while tailoring SBTW.

Chapter 2

Underwater Modal Testing of 1D Beam

2.1 Introduction

In the earlier chapter, the differences between different types of mechanical waves were discussed. The first step in generating traveling waves is to modal test an aluminum beam immersed in water and then, investigates the propulsive characteristics of structure-borne traveling waves in this beam.

2.2 Modal Testing Setup

The **Figure 2.1** and **Figure 2.2** shows an experimental setup was designed and fabricated using 80:20 aluminum structures to support the equipment for modal testing. This supporting structure holds a Polytec OFC 040 Scanning unit, a Polytec PDV 100 single-point laser vibrometer, and two Modal Shop's smart shakers. A glass water tank of 10 gallons was used to represent the quiescent water environment for underwater testing. A small setup was created inside the water tank to create a straight pathway for the object to travel over the surface of the water. A 6061 Aluminum beam with a dimension of 381mm x 25.4mm x 0.635mm was attached to the two shakers using a 254mm threaded rod.

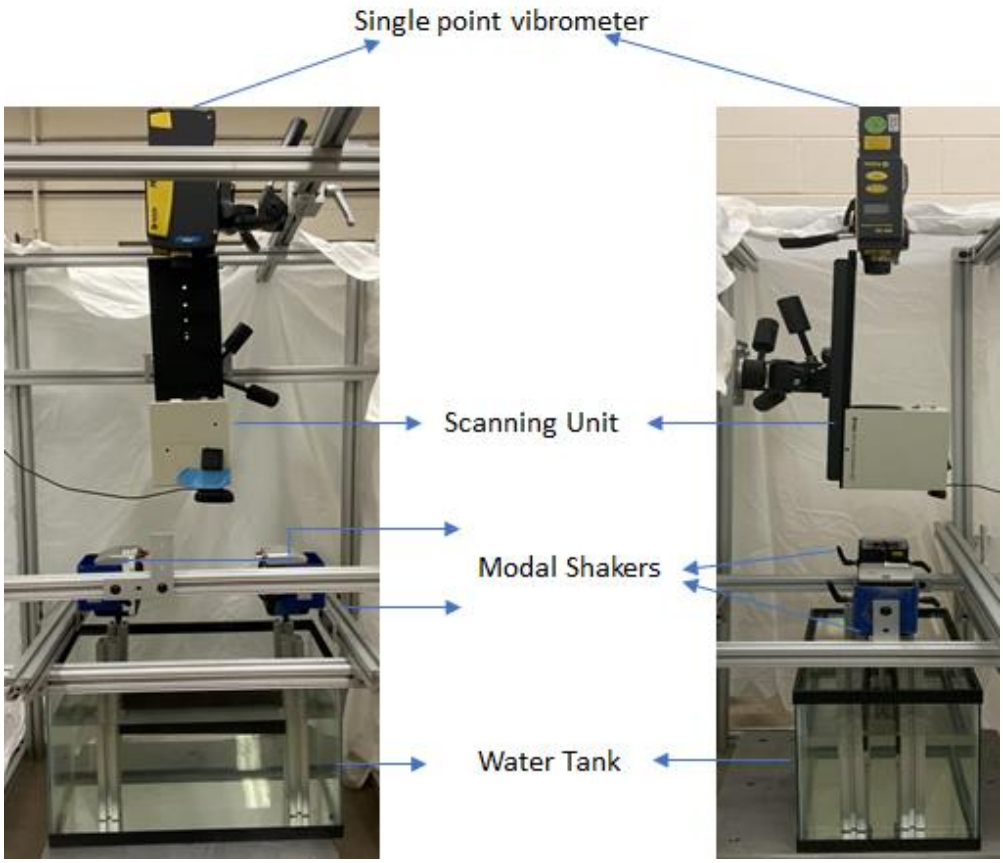

a) ***Front View*** ***b) Side View***

Figure 2.1: Experimental setup for SBTW generation and modal analysis

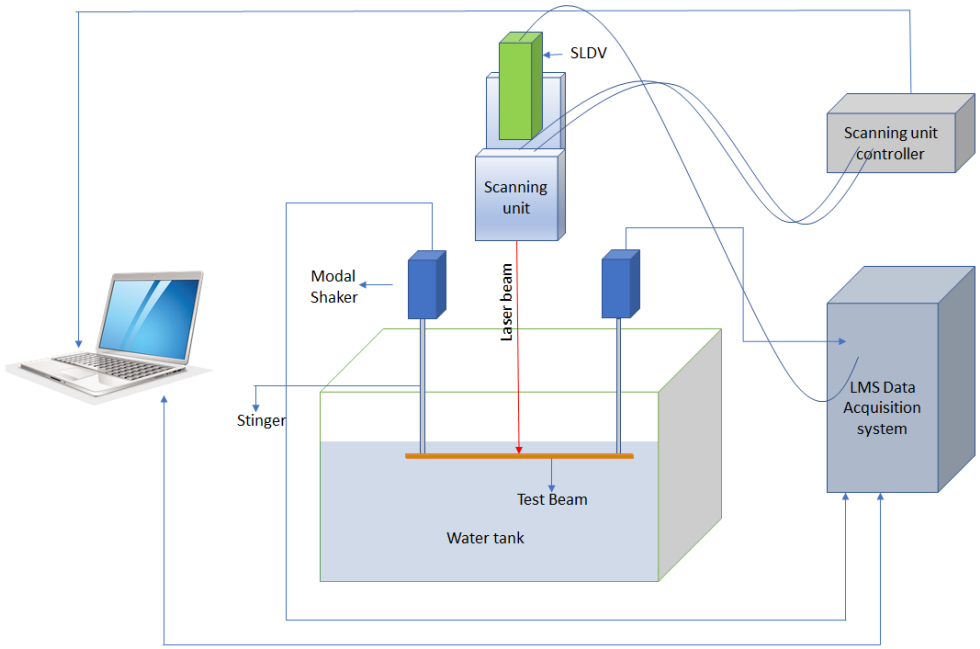

Figure 2.2: Schematic of experimental setup for SBTW generation and modal analysis

2.2.1 Boundary Conditions

In every dynamic's testing, boundary condition plays an essential role. In the current setup, a pinned – pinned boundary condition was applied on the aluminum beam. The boundary condition is imposed by stingers attached to the ends of the beam. The overall length of the beam selected was 381mm. Two stingers of 355.6mm were initially superglued to be beam with 25.4mm from the two ends of the beam. The other ends of the stingers were attached to the shaker. However, as superglue was not effective underwater, two threaded rods of 10 – 32 x 10 inches were then bolted to the beam at the locations shown in **Figure 2.3**.

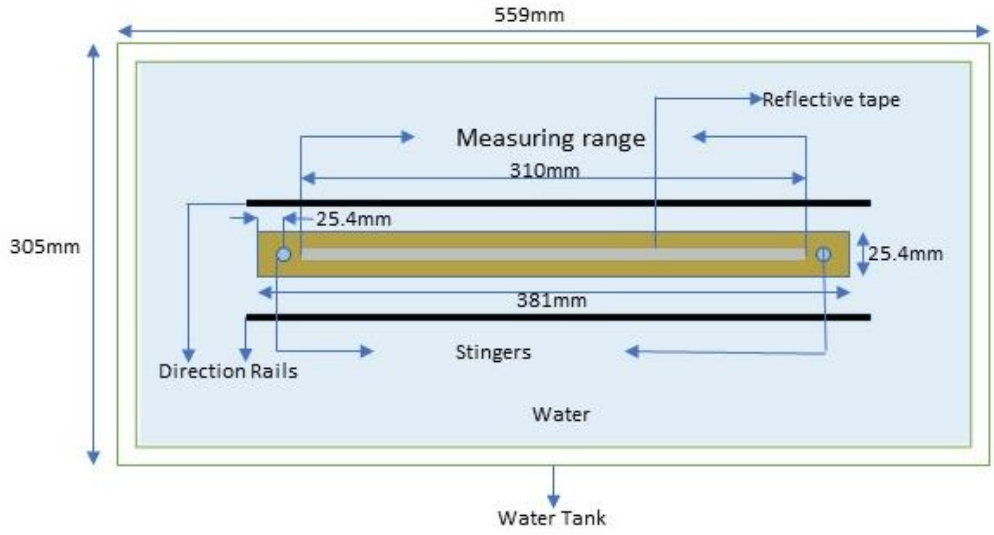

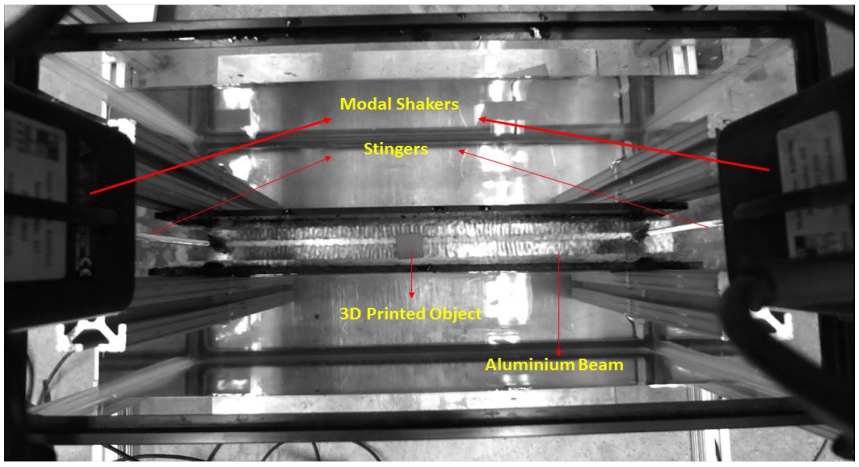

Figure 2.3: *Underwater beam setup in the water tank*

While performing modal analysis, it is necessary to align the beam and the shakers properly to avoid any residual stresses in the beam [24]. So, in this setup, the distance between two shakers needed to be the same as the distance between two holes in the test beam so that the force exerted from the shaker through the stingers should be exactly perpendicular to the surface of the beam.

2.2.2 Water Height over the Beam

Water height is an important aspect of this testing. As we increase the water height over the surface of the aluminum beam, the damping, mass, and stiffness acting on the beam would also increase. So, after a few trials, the height of water over the surface of the beam was maintained at 15mm. The depth of water below the beam was 216mm. **Figure 2.4** below shows the height of water over the beam.

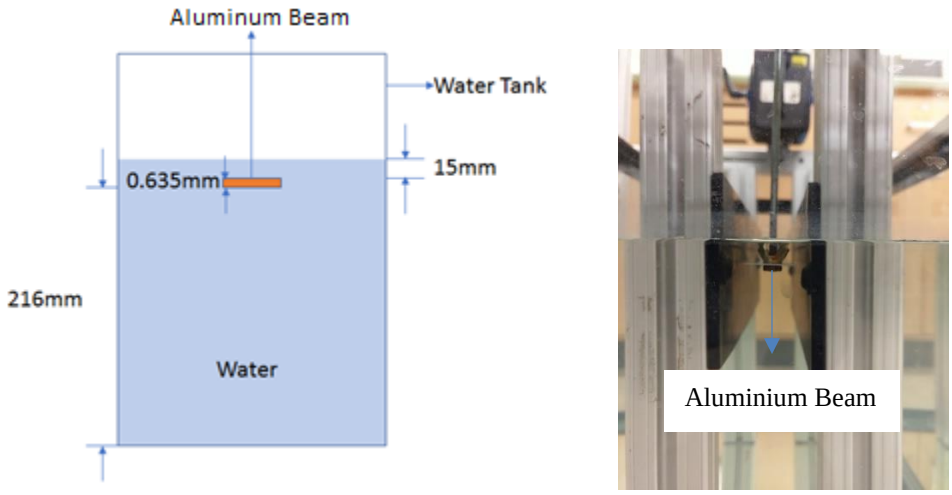

a) ***b)***

Figure 2.4: a) *Schematic for the depth measurement of beam immersed underwater.* ***b)*** *Test setup showing the test beam from side view*

2.2.3 Scanning Laser Vibrometer setup

To simulate a traveling wave on a 1D beam, the system needs many spatial points over the beam. These spatial points provide the behavior of a particle under forced vibration at a particular location. To have a very smooth wave plot, the beam was divided into 31

testing points, each 10mm apart from the other. But, due to equipment constraints, the test setup had a single-point laser vibrometer. To measure the vibrations at all 31 points, the Single Laser doppler Vibrometer (SLDV) had to be moved manually to the desired location. This process was time-consuming and moving the laser for every point would disturb the beam setup giving noisy results. To eliminate the problem, we integrated a scanning unit with the SLDV to automate the process of positioning the laser at the desired location without disrupting the setup. So, a Polytec OFC 040 Scanning unit was selected to integrate it with the SLDV. The scanning unit consisted of two mirrors which were operated by two stepper motors to control the direction of the laser point in the X and Y plane. A MATLAB Application was developed to control the scanning unit, which included Calibration, Image capturing, live video functionality, and adjustable ruler for the X and Y planes.

The working of this assembly was quite straightforward, SLDV was concentrically aligned with the upper portion of the scanning unit, and the location of the laser was controlled by MATLAB application. A webcam was attached to the scanning unit for observing the live locations of the laser point. So, this was a successful effort to minimize the energy to move the SLDV manually at every point. The setup also helped in reducing the noise in signal data giving a clean frequency response function (FRF).

2.3 Modal Testing

As discussed in chapter 1 regarding the generation of SBTW, mode shapes and FRFs are obligatory in the selection of a frequency between two consecutive natural frequencies. The selected frequency would be used to generate the traveling waves.

To perform the modal testing, firstly, the SLDV and the two shakers were connected to Siemens's LMS data acquisition system. Then the scanning unit was integrated with a single-point laser vibrometer. As the two-force input method was used for SBTW generation, a multi-input multi-output (MIMO) FRF test was performed from Siemen's test lab to acquire response of beam while excited from both the shakers alternatively for each point.

2.3.1 Modal Test Specifications

After configuring all the settings, such as setting up proper connection and sensitivity in the LMS test lab for all the equipment are attached, the frequency spectrum and signal are selected. SBTW uses the resonant properties of a material for thrust generation underwater. So, to attain a higher thrust to move an object underwater, the system needs to work on low-frequency bandwidth. The lower frequency range provides the maximum thrust required to generate undulatory motions underwater. Keeping this concept as a reference, 0Hz to 1024Hz frequency measurement range was selected with 4096 spectral lines.

Selecting a correct signal for excitation of actuators is very important in modal analysis. For a shaker test, an excitation signal is selected such that there is minimum leakage and no need to use window functions. So due to this, the modal test was performed using the chirp signal for 40 averages. The FRF measurement was performed by giving a signal to shaker 1 for point 1 and then to shaker 2. The process continued for all 31 points. The FRF data files were converted to MATLAB for post-processing.

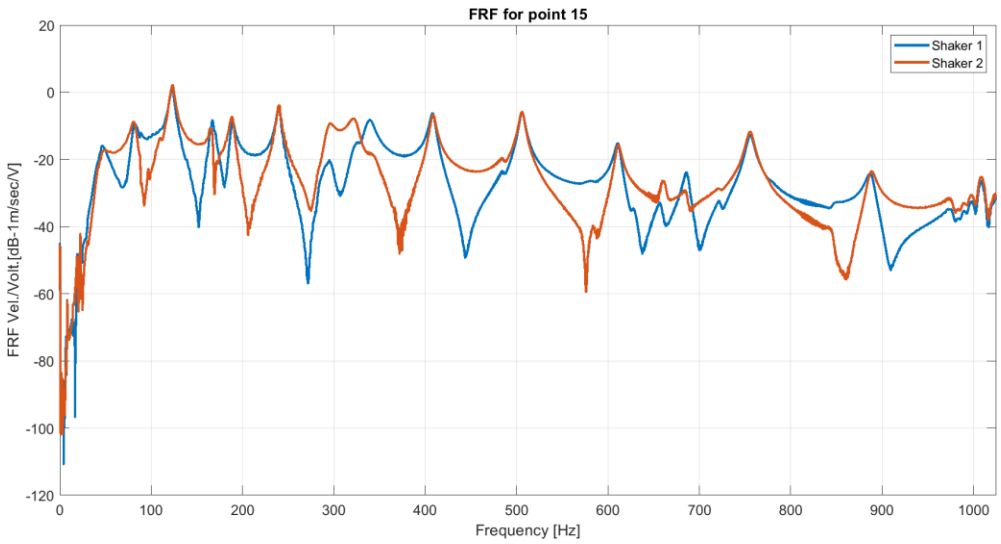

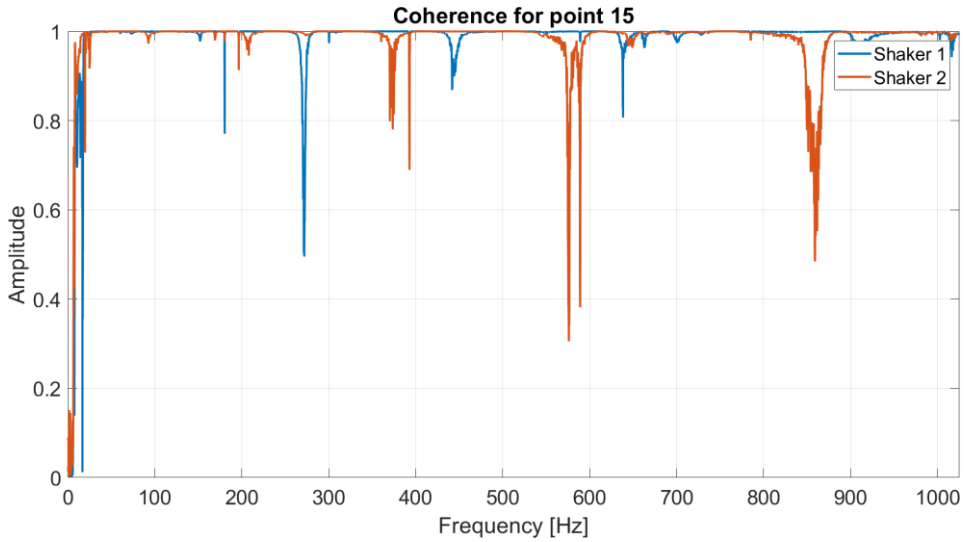

Figure 2.5: *FRF and Coherence for shaker 1 and shaker 2 measured for point 15 on the beam*

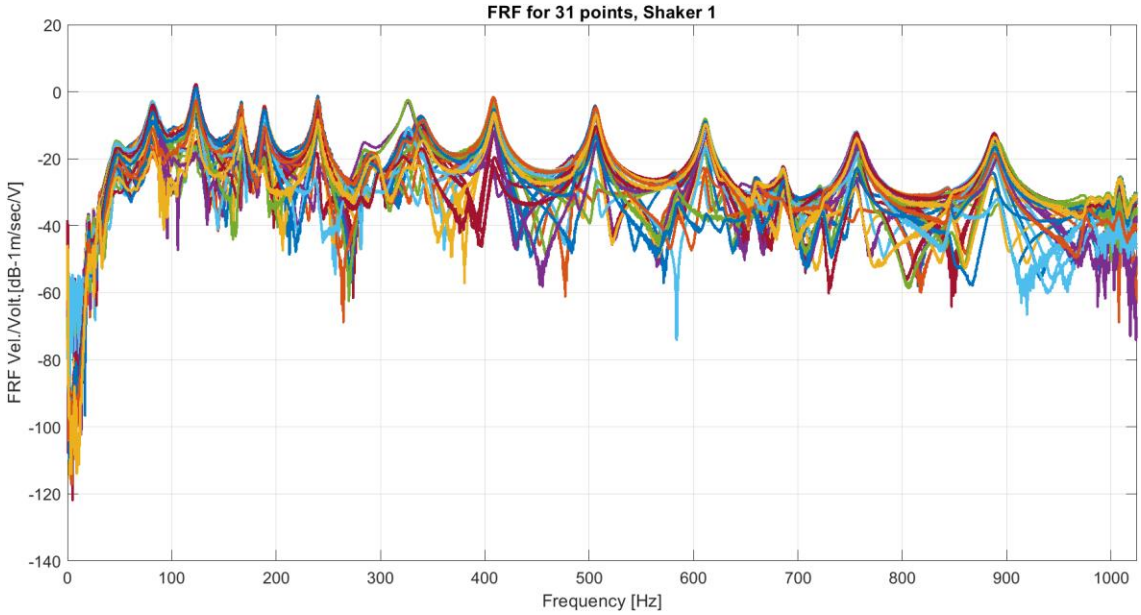

Figure 2.6: *FRF measured for all 31 points on the beam for shaker 1*

Figure 2.5 shows the overlapped FRF for shaker 1 and shaker 2 showing the similarity between natural frequencies after exciting the shakers individually for modal testing. It could be observed that all the natural frequency peaks are matching in both cases of actuation confirming that the signals given by shakers while testing were similar. **Figure 2.6** displays all the FRFs measured for 31 points marked on the test beam 10mm apart while exciting shaker 1. Similarly, **Figure 2.7** shows the FRFs for the second shaker. These two FRF plots from shakers 1 and 2 are further used to locate prospective frequencies for SBTW generation. In the next chapter, these FRFs will be used to simulate the test condition while acquiring wave envelops plot for structure-borne

traveling waves. But before moving forward it is necessary to validate if the natural frequencies acquired from modal testing are correct.

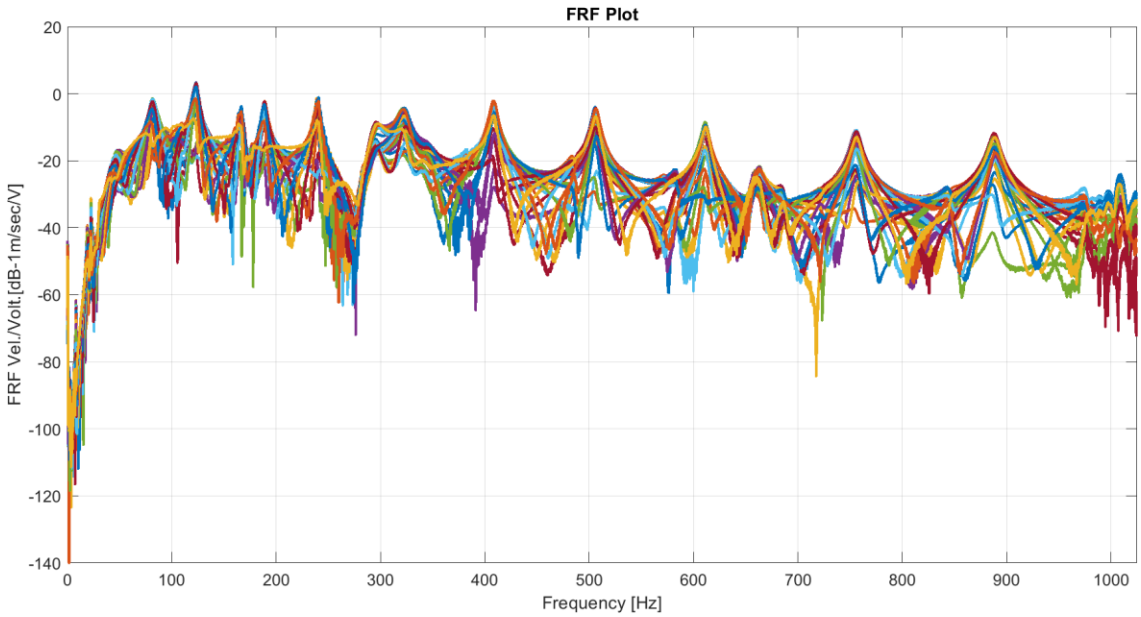

Figure 2.7: *FRF measured for all 31 points on the beam for shaker 2*

2.4 Modal Test Validation

This section focuses on acquiring operating deflection shapes using the previous FRFs by a numerical method in MATLAB. Then the mode shapes are used to perform a modal assurance analysis to validate if the mode shapes are not dependent on the operating deflection shapes from other frequencies.

For this validation process 2nd to 10th natural frequency values were obtained from the FRFs shown in **Figure 2.8**. These 9 natural frequencies were used to plot the operating deflection shape (ODS) of the beam. The figures below are ODSs for respective natural frequencies.

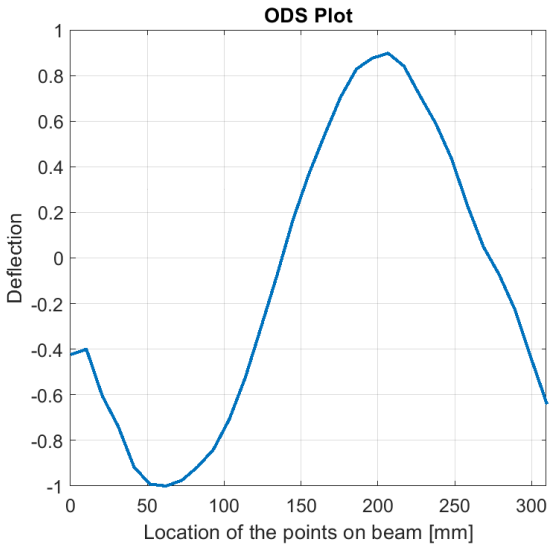

a) *2nd ODS shape at 8.25Hz*

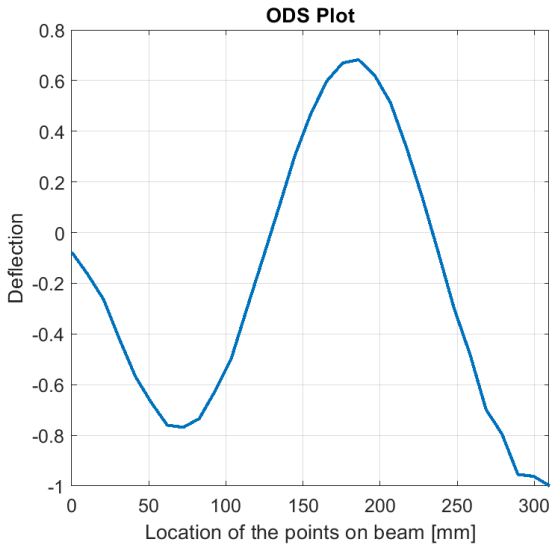

b) *3rd ODS shape at 23.75Hz*

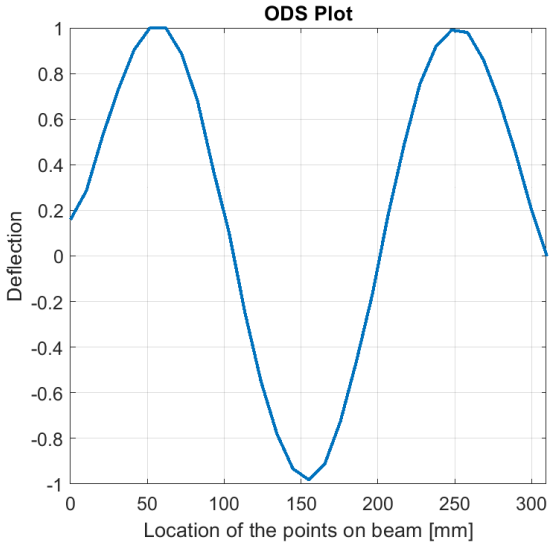

c) *4th ODS shape at 47Hz*

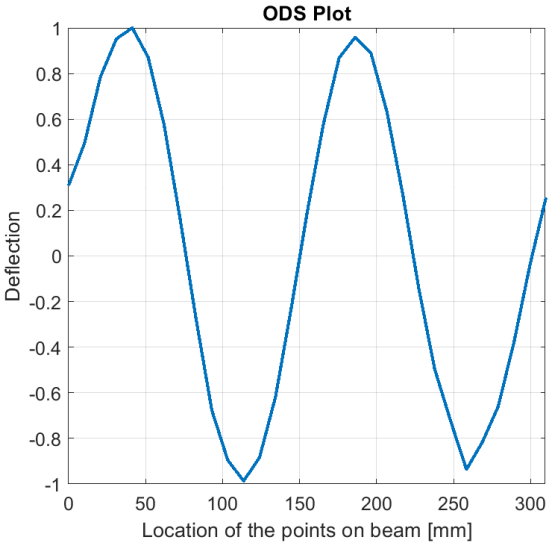

d) *5th ODS shape at 81.75Hz*

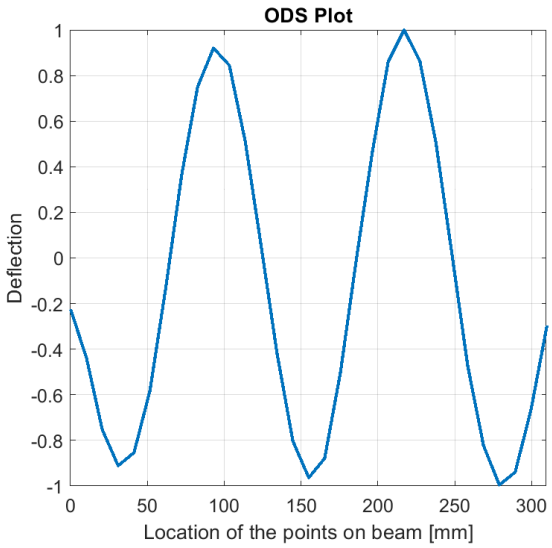

e) *6th ODS shape at 122Hz*

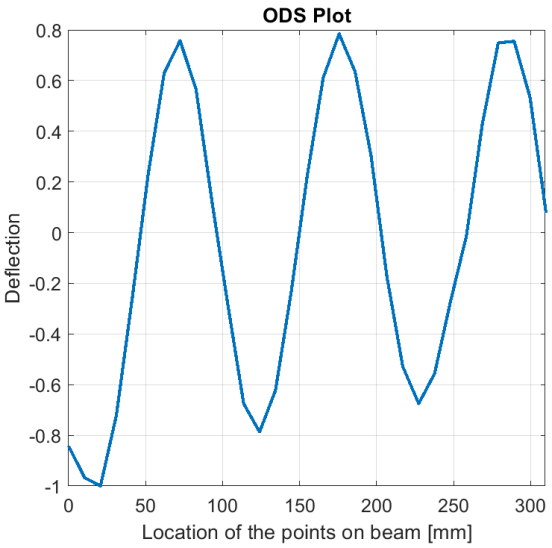

f) *7th ODS shape at 166Hz*

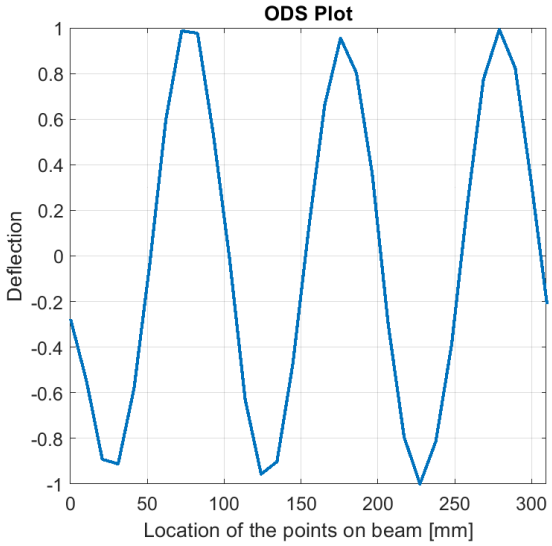

g) *8th ODS shape at 188Hz*

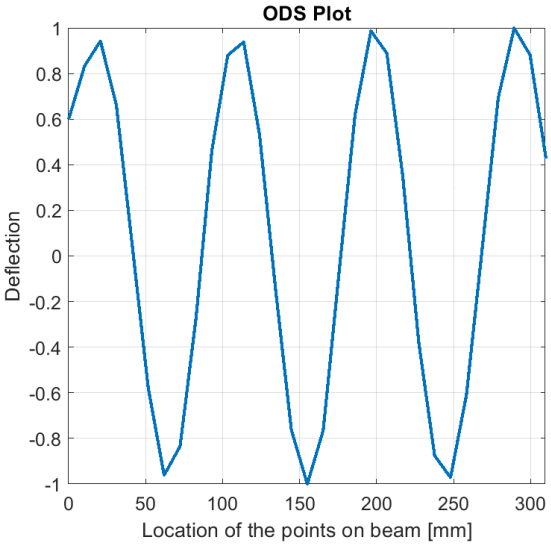

h) *9th ODS shape at 239Hz*

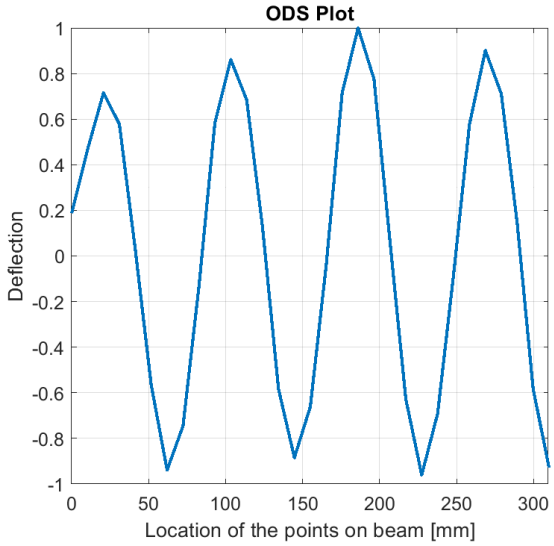

i) *10^{th} ODS shape at 296Hz*

Figure 2.8: *ODSs of aluminum beam from 2^{nd} to 10^{th} natural frequency*

These Operating deflection shapes were used to perform a Modal assurance criterion (MAC) analysis to check if the natural frequencies and FRF acquired from modal testing are credible or not. This validation is important because the further part of this research only deals with the ODS and frequencies attained in modal testing. To get the best possible SBTW for propulsive effects, the natural frequencies should be accurate. The MAC matrix compares simulated ODSs with itself to show the correlation between them and the contribution in different ODS. In this case, only the 4th mode shape to 10th mode shapes was considered for this analysis. As to generate favorable SBTWs, lower frequencies such as below 50Hz have more resonating force than higher frequencies creating turbulence in the water. So, the favorable region for TW was from 60 to 300Hz. Due to this the lower frequencies are skipped in MAC analysis.

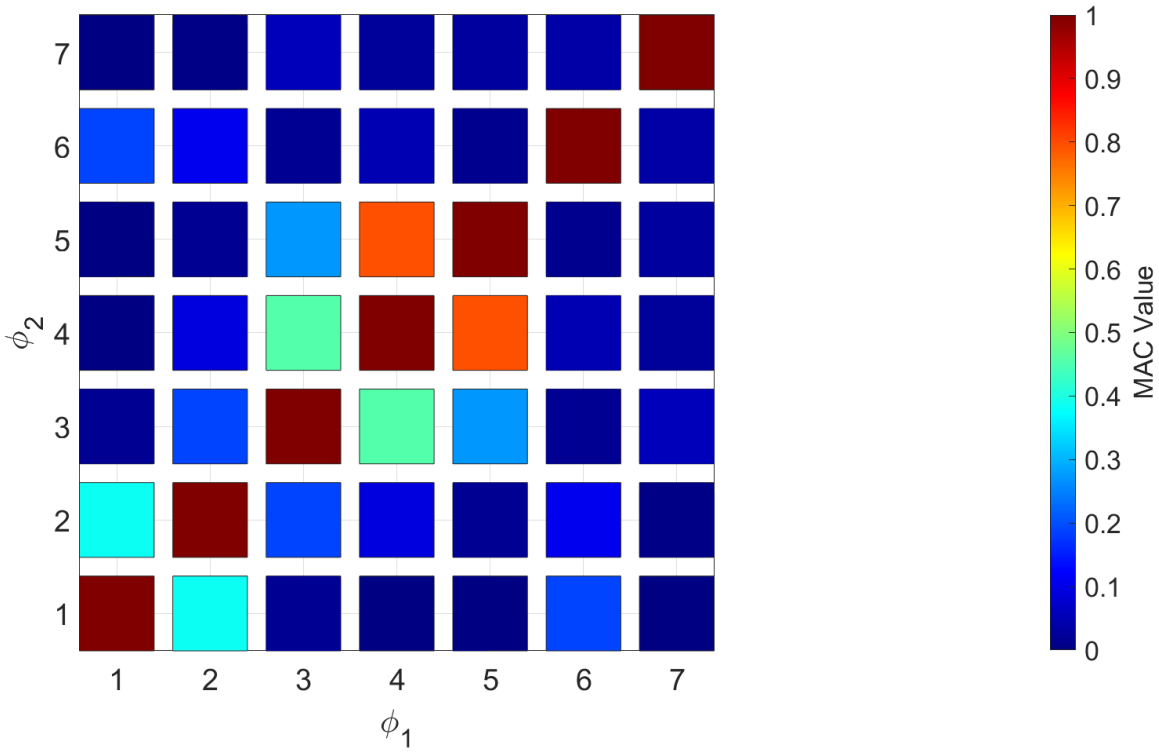

Figure 2.9: *Modal assurance chart comparing simulated vs experimental mode shapes*

Figure 2.9 shows the MAC chart where it can be clearly observed that for most of the cases the diagonal is very well isolated than the other ODS. The only ODS with a considerable contribution with a different ODS is 188Hz. The MAC suggests that they might be very similar. But due to lack of spatial points they cannot be isolated properly. But, the rest of data is acceptable and this gives us the validation that the experiment was successful with high-quality results. The small errors between theoretical and experimental mode shapes could be due to inaccuracies in testing conditions including signal noise, pre-stress material, and boundary conditions.

2.5 Conclusion

The main objective of this chapter was to construct a setup capable of generating structure-borne traveling waves and to obtain natural frequencies and mode shapes for further research. In this chapter, a sturdy setup was constructed which could hold a laser vibrometer, scanning unit, two modal shakers, and the test beam. A 389mm length of the thin aluminum beam with a thickness of 0.635mm was selected for this test and pinned–pinned boundary conditions were applied. The stingers were bolted to the beam from one end and the other end was connected to the two shakers. An experimental Modal test was performed to obtain FRFs from both the shakers for post-processing. Using those FRFs mode shapes were plotted to verify the natural frequencies. To conclude the modal testing and demonstrating high-quality results a MAC analysis was performed to check the correlation between simulated and experimental mode shapes.

Chapter 3

Structure Borne Traveling Wave Generation in Underwater Beam

3.1 Introduction

The earlier chapter was concerned with modal testing of a beam for obtaining mode shapes and FRF for the generation of traveling waves (TWs). This chapter was developed to explore the generation and working of traveling waves under water, using two forces input method. Researchers have proven in their study that structure-borne traveling waves are tailored by simultaneously exciting the test structure by two-point forces [25].

This experimental research has used two modal shakers to excite the aluminum beam simultaneously. The voltage signals applied to the shakers use a frequency lying midway between the two consecutive modes shapes frequencies or resonant frequencies with a phase difference of 90 degrees.

The initial part of this chapter would deal with simulating traveling waves in the FE beam model using a response function to test a frequency for prospective traveling waves using the data of experimental modal analysis. The simulation would also optimize phase angle for better traveling wave quality which is validated through a cost function.

As the chapter moves forward, the simulation is experimentally validated by generating underwater SBTW's using the test frequencies from the results of the simulation. An

observation is also made on the effect of propulsive forces generated from SBTW's over the object. The data of all these experiments are collected and a test validation is performed to prove if the flow of water is caused by traveling waves.

3.2 Numerical Simulation of Underwater Traveling Waves

The finite element modal developed for this research represents a thin 1-dimensional aluminum beam pinned-pinned at both ends by stingers from modal shakers. **Figure 3.1** shows the experimental beam model used to validate the response from the simulation. The aluminum beam has a dimension of 381 × 25.4 × 0.635mm (15 × 1× 0.025in.). The two shakers are visible which are used as actuators for two input methods to generate traveling waves.

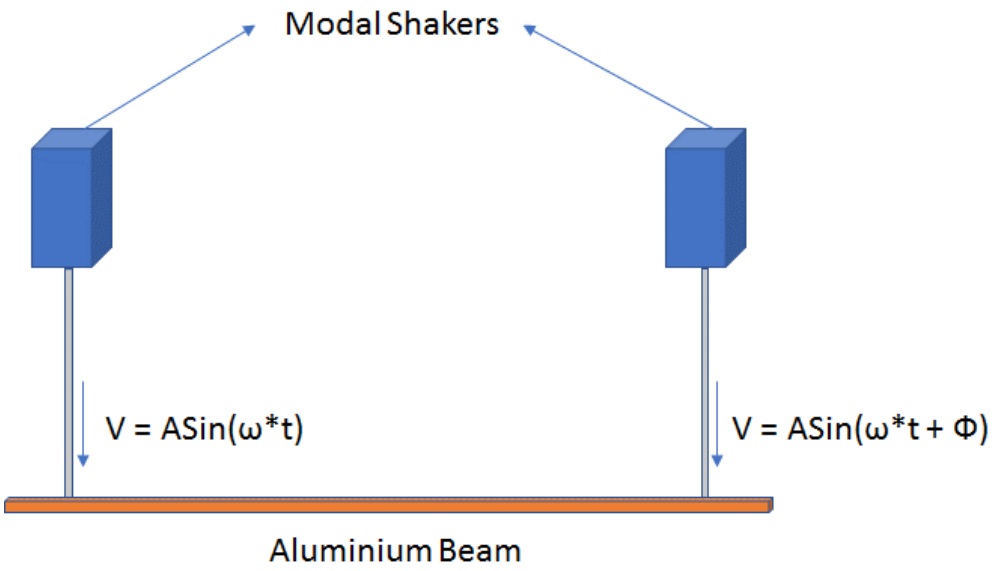

Figure 3.1: *SBTW setup schematic using two force input method*

Figure 3.2 shows the frequency response of aluminum beam from 30Hz to 350Hz spectrum due to excitation by shaker 1. Shaker 1 and shaker 2 yields almost the same results as the location of excitations are symmetric. The frequency response is defined as the ratio of the beam velocity measured through SLDV to the input voltage given to shakers. The natural frequencies are denoted by dotted lines on the peaks in the figure.

The regions between these consecutive natural frequencies lies are the prospective frequency that could generate traveling waves. The region from f4 – f10 frequency is selected as the optimum range for traveling waves where propulsive forces could be used to move an object underwater. f4 natural frequency in this plot is the 3rd mode shape of the beam and f10 is the 9th mode shape.

Table 3.1: *Natural Frequencies of the system for selected region*

f4	f5	f6	f7	f8	f9	f10
47Hz	81.75Hz	122.75Hz	166Hz	188Hz	239Hz	296Hz

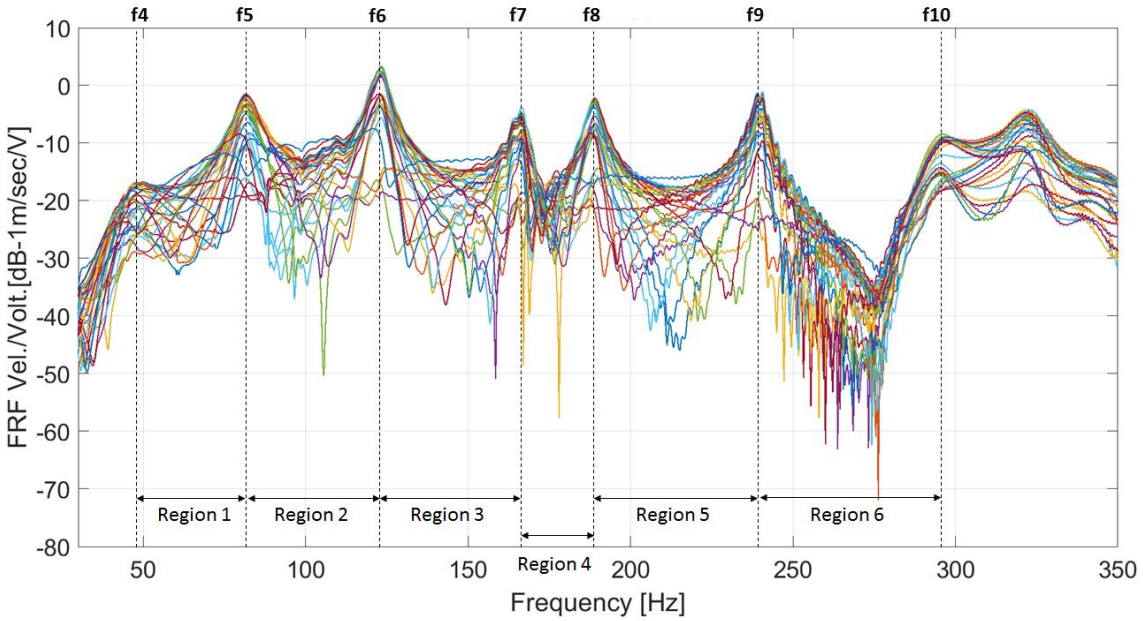

Figure 3.2: *Frequency response function for potential regions to generate SBTW*

3.3 Structure borne traveling wave generation

As mentioned in chapter 1, the structure-borne traveling waves are generated by harmonically exciting the aluminum 1D beam using two symmetrically located actuators at the same frequency (f) but with a phase difference of ϕ. This is implemented for the two shakers shown in **Figure 3.1** using the same voltage amplitude of V. After the forces are applied, the SBTW's are generated through super positioning the response from each shaker.

Harmonically exciting a single actuator would result in a specific operating deflection shape depending on the location of the actuator, the nearby participation of mode shapes, and the frequency of excitation. So, when both the shakers are excited using the same

frequency, the resulting operation deflection shape is the superposition of the response of individual ODSs from each shaker. The main factor resulting in the desired superposition of ODSs and causing traveling waves is the phase offset maintained through the input signal of the actuators.

The force input from shaker 1 is shown as $V1 = A*\sin(2*\pi*f)$ and force input from shaker 2 is $V2 = A*\sin(2*\pi*f \pm \phi)$. Therefore, the superposition of these two forces to generate traveling wave is shown as:

$$SBTW = A*\sin(2*\pi*f) \pm A*\sin(2*\pi*f \pm \phi)$$

The phase offset between the two-voltage signals to the actuators determines the quality of traveling waves. A normal Structure borne traveling wave is a combination of traveling and standing waves and as the quality of SBTW is increased, the standing wave component from it is reduced. The quality of the traveling wave is estimated or evaluated through the method of the cost function [3]. The cost function determines the weightage of the standing wave or traveling wave component in the SBTW.

To determine the quality of SBTW, wave envelopes of these waves are observed i.e., the plots where the area is swept by the wave over time. In a wave envelop a constant wave with no changes in amplitude of the displacement over a period shows a pure traveling wave. But a sharp nodal point that has zero displacements in a wave envelope shows a pure standing wave. The SBTW's generated experimentally are usually hybrid waves where there is no nodal point where the displacement is zero or and a varied deflection.

The cost function is calculated by finding the minimum and maximum absolute values of the wave envelope. Consider the maximum value as Ymax and the minimum value as Ymin. So, the equation for cost function is written as:

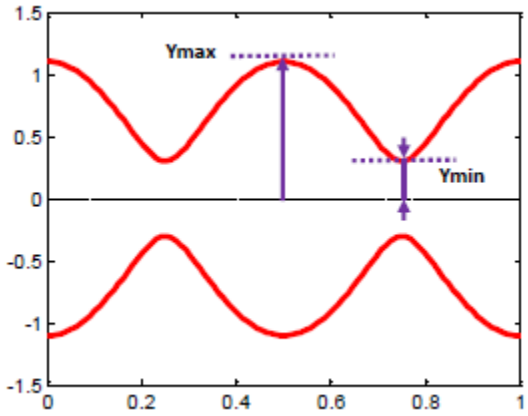

$$CF = \frac{Y_{max} - Y_{min}}{Y_{max} + Y_{min}}$$

Figure 3.3: *Simulation TW wave envelop for 67Hz frequency*

The value of the cost function near 1 corresponds to a standing wave and the value of the cost function near 0 corresponds to the traveling wave. To generate a good quality of traveling wave for propulsive forces, the cost function should lie between 0 to 0.3.

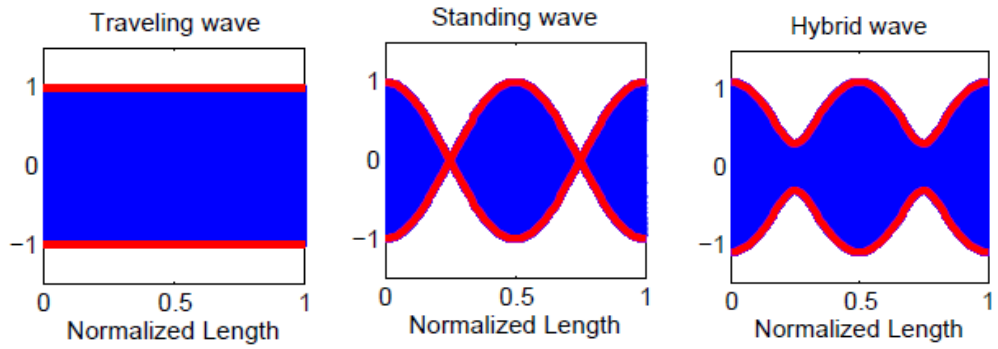

Figure 3.4: *Simulation TW wave envelop for 67Hz frequency*

3.3.1 Simulating Wave envelopes for SBTWs

To verify the theory for prospective traveling waves in the region selected from the FRF plot, a MATLAB code was developed to find the beam response of any excitation frequency used as a signal input to both the actuators. The MATLAB code used the FRFs from both the actuators for all 31 points to generate a response wave plot. According to the theory a frequency is chosen between two consecutive natural frequencies and is used to excite the actuators keeping the same voltage amplitude but with a phase offset and the superposition of the response waves from both the actuators would result in a structure-borne traveling wave.

The MATLAB code is built on the same theory, a frequency exactly between 3rd and 4th mode shape is chosen as test frequency. Then this frequency is used to excite the actuators through the 31 points experimental FRFs. A phase term is multiplied with the second actuator which is optimized for the best possible cost function at that frequency. Then the wave envelope is plotted adding the response from both the actuators. This process is continued for all the regions mentioned in **Figure 3.2** for prospective traveling waves.

3.3.2 Phase offset Optimization

There is an optimized phase offset for each excitation frequency which would yield high-quality SBTW. The value of phase offset varies from [0^o, 180^o]. The phase offset is dependent on the location of the actuator and the nearby mode shapes of the excitation frequency. To optimize the phase angle, the Optimization toolbox was used in MATLAB

where the response of actuators was evaluated, and then the trials were performed to optimize phase angle against the value of cost function. The phase angle was iterated till the optimization toolbox finds a minimum value for cost function at that excitation frequency.

3.3.3 Results

Using the above procedure, first the **67Hz** frequency was chosen which was exactly between the 3rd and 4th mode shape. The wave envelope response for 67Hz is shown in the **Figure 3.5**. So, it was observed that this is hybrid wave and the cost function for this plot was **0.15** and the optimized phase angle was **99.57°.** After observing the wave plot, the participation of 3rd mode shape can clearly be there are three humps in the plot.

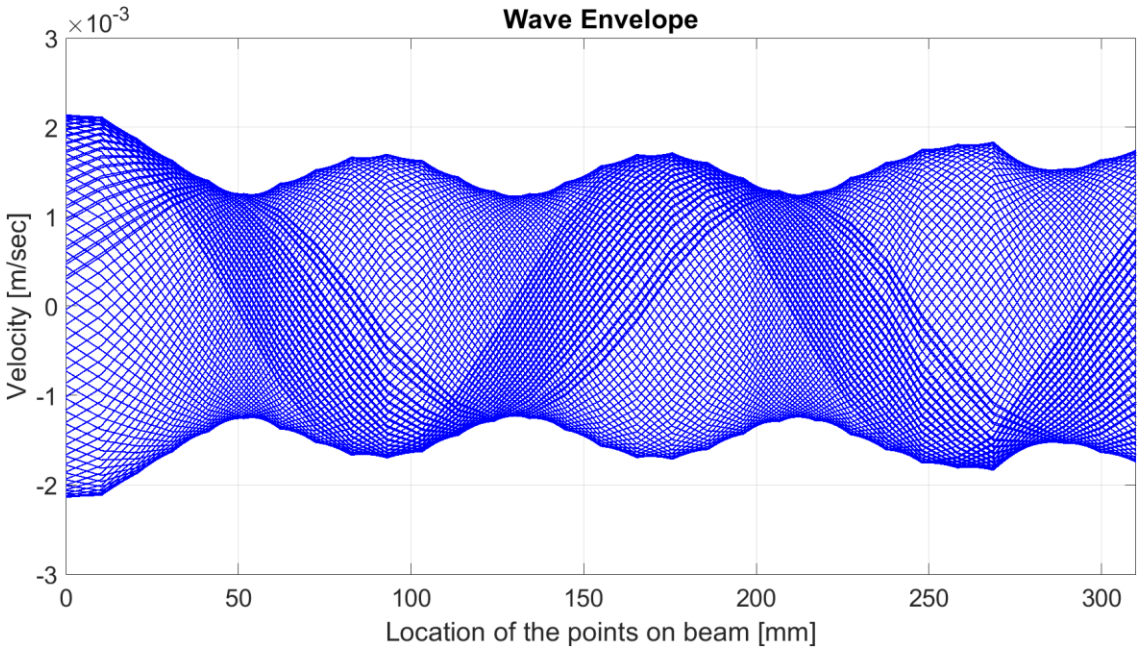

Figure 3.5: *Simulation TW wave envelop for 67Hz frequency*

From the region 2, **104Hz** was selected as excitation frequency which was exactly between the 4th and 5th mode shape. The wave envelope plot is shown in the **Figure 3.6**. The cost function calculated for this plot was **0.17** at a phase angle of **63.89**^{o}

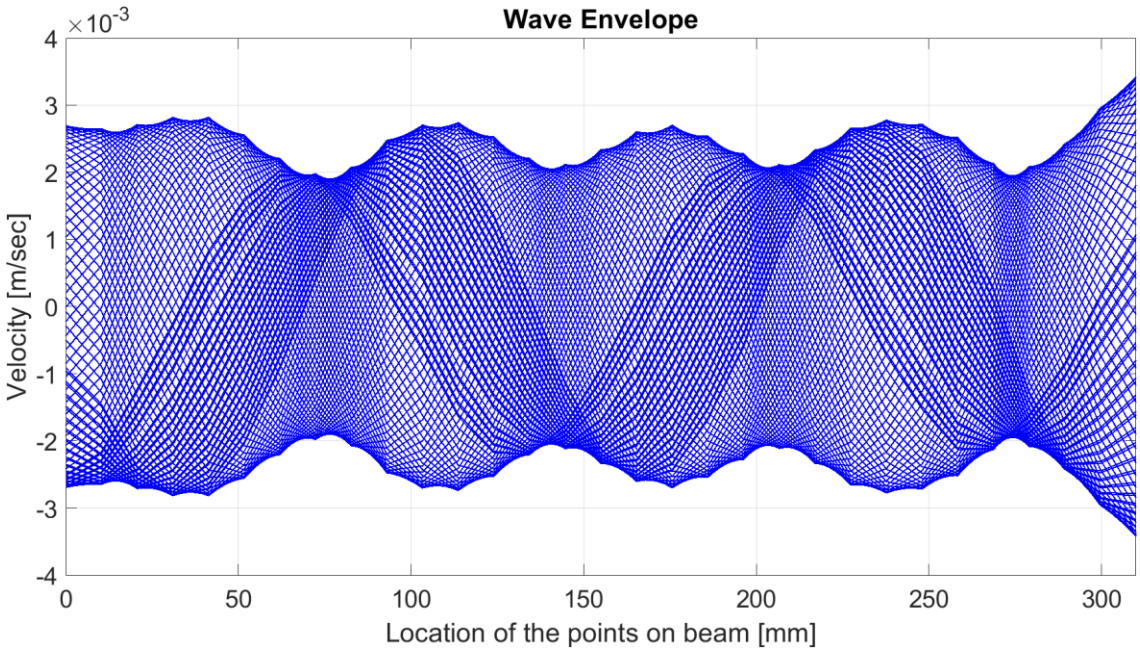

Figure 3.6: *Simulation TW wave envelop for 104Hz frequency*

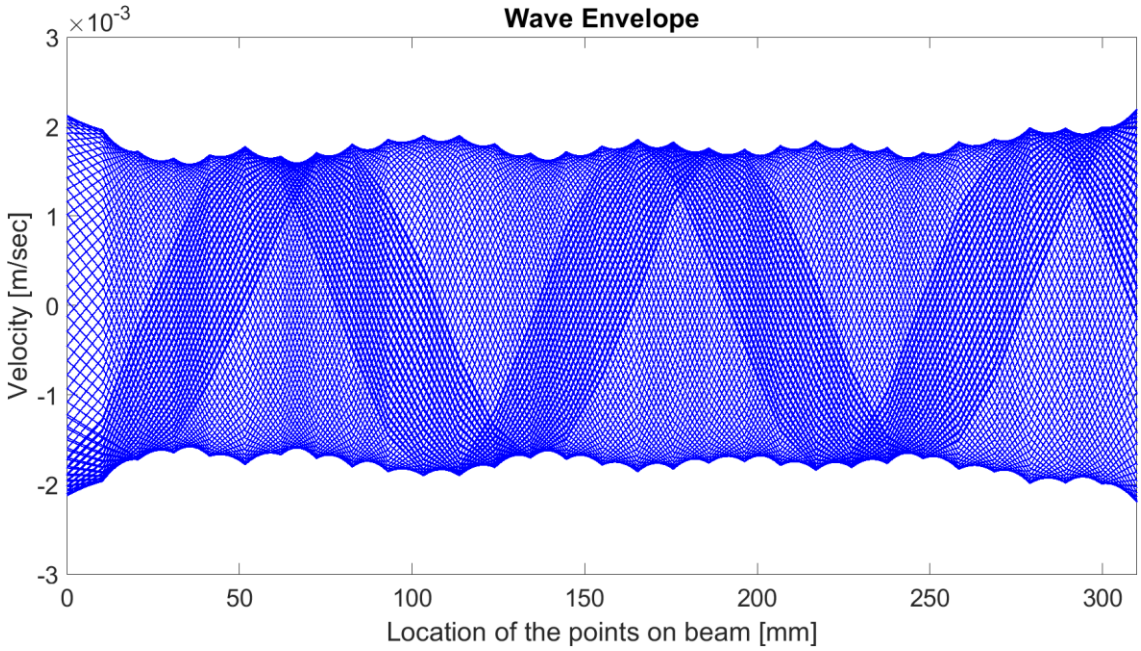

Figure 3.7: *Simulation TW wave envelop for 147Hz frequency*

The wave plot shown in **Figure 3.7** is evaluated for **147Hz** frequency was the best SBTW plot, as the cost function was just **0.07** which had a very less amount of standing wave component. The phase offset for this case was optimized to **93.86**°

In this case **179Hz** frequency was selected from region 3 between the f4 and f5 frequencies. This SBWT has the maximum effect of standing wave in it as the cost function is **0.35.** The phase offset optimized for this case is **100.80**°**.** Envelope

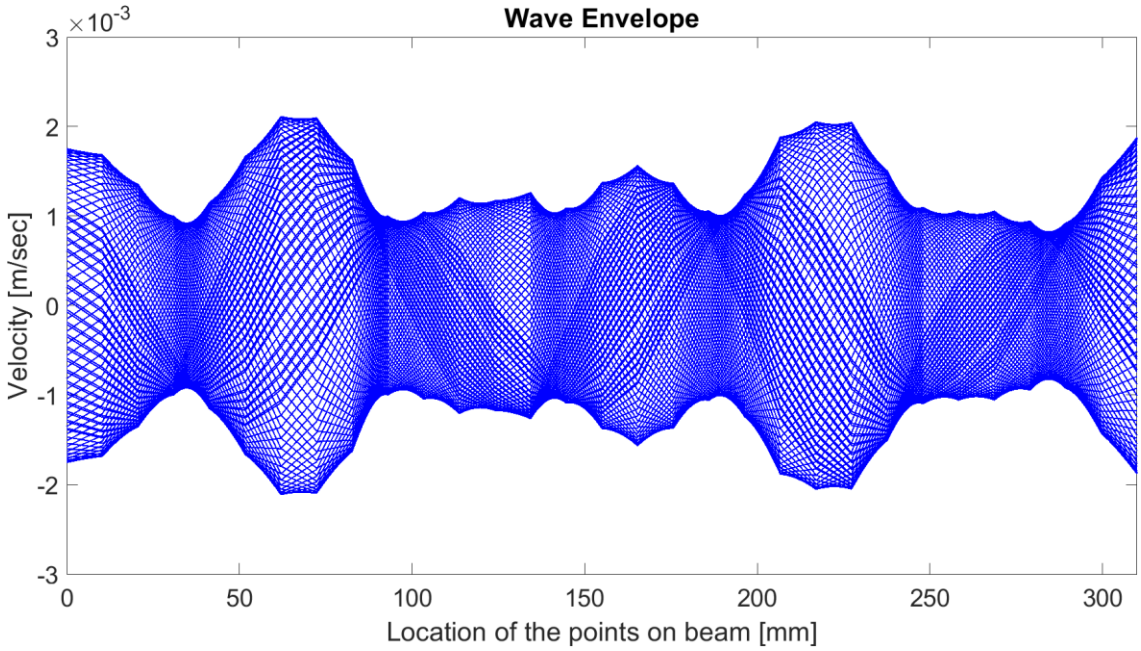

Figure 3.8: *Simulation TW wave envelop for 179Hz frequency*

Same goes for this case, **270Hz** frequency was selected as excitation frequency for the actuators from region 6 between 8th and 9th mode shapes. We can clearly observe the effects of 8th mode shape in the wave plot. The cost function evaluated for this wave plot was **0.30** for a phase angle of **122.43**$^{\circ}$. For this SBTW, the standing wave component is more prominent than the traveling wave component which is affecting the value of cost function.

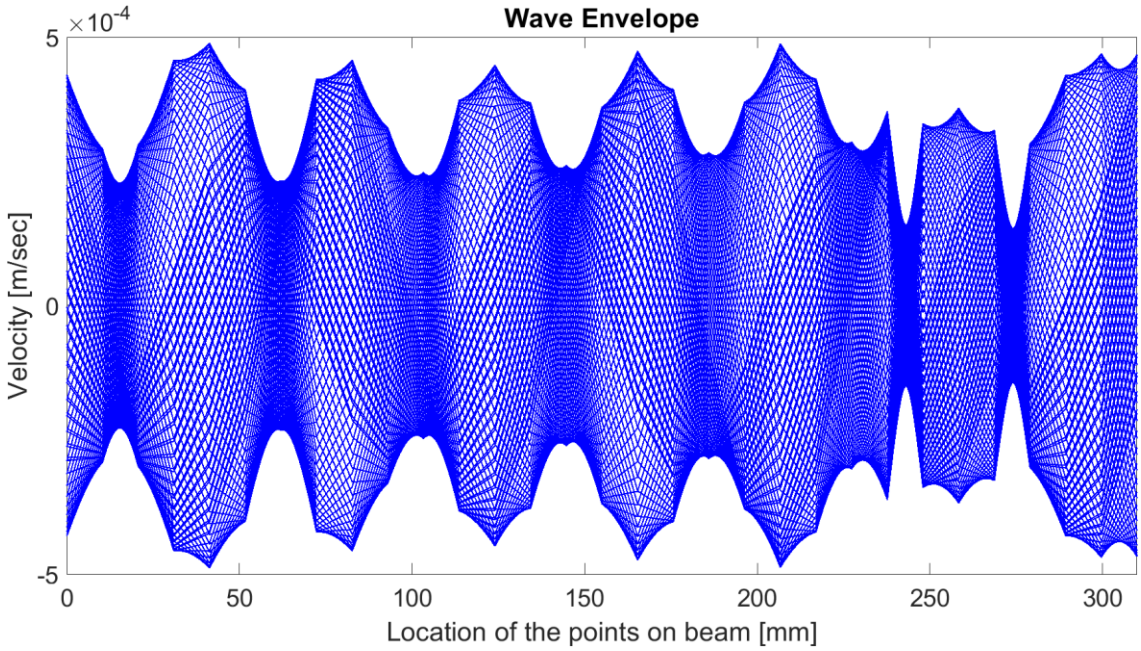

Figure 3.9: *Simulation TW wave envelop for 270Hz frequency*

3.4 Experimental Generation of Structure Borne Traveling Waves

To validate the previously developed theory FE model for simulating wave plots of SBTW's, an experimental setup was developed for testing. The testing setup is discussed in the 2nd chapter. To test the credibility of this theory a sinusoidal voltage sweep was applied to both the modal shakers simultaneously using Siemen's data acquisition system (LMS) as a signal generator. The excitation frequencies selected for this test were the same as in the simulation. The voltage amplitude was decided according to the resonance force of each frequency. It is understood that low frequencies have high resonance force so, if we keep the voltage in optimum range then the setup won't get disturbed. As all the frequencies selected were exactly in the middle of two consecutive natural frequencies so, the phase offset was chosen as 90^{o} for every case.

As both the shakers are excited, the velocity of the beam at all 31 points is measured. The frequencies used for generating traveling waves are the same as that of simulation. The voltage amplitude for all the waves was kept at 0.01V. After measuring the velocities for each point at each frequency, the data was converted into MATLAB. The MATLAB data was then post-processed to plot a velocity wave envelop of the beam velocity to validate if the wave generated is an SBTW.

Figure 3.10 shown below is the experimental setup for generating SBTWs. It could be observed that between the black rails water has some wave-like motion. This motion is a structure-borne traveling wave at 67Hz excitation frequency with a 90º phase offset

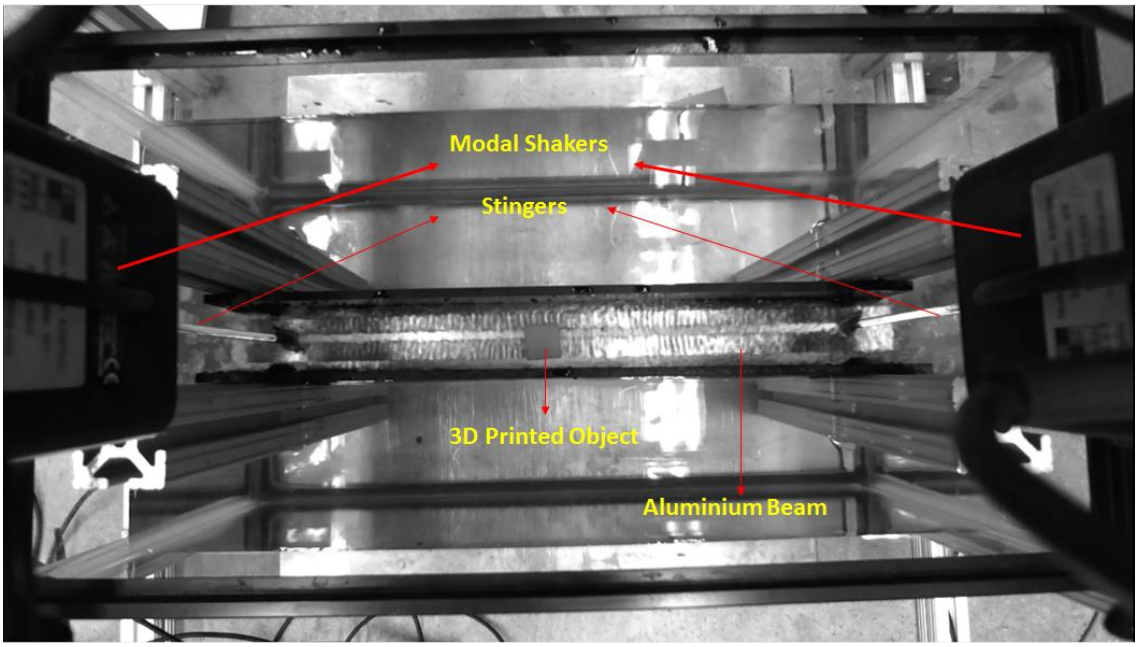

Figure 3.10: *Experimental Setup to generate SBTW using two smart shakers as actuators (Top View)*

3.4.1 Experimental Validation

The velocity data acquired from the test setup needs to be validated to prove if the generated waves were traveling waves. So, the rms values of velocity for each point are plotted against the beam point locations. So, below are the velocity wave plots for all the excitation frequencies used to generate SBTW.

Figure 3.11 a show the wave envelops for **67 Hz** frequency with a phase offset of **90º**. It can be observed that the simulation wave envelops, and experimental wave envelop are similar. They both have an effect for 3rd mode shape in their wave plot. The evaluated cost function for this frequency is **0.1910.**

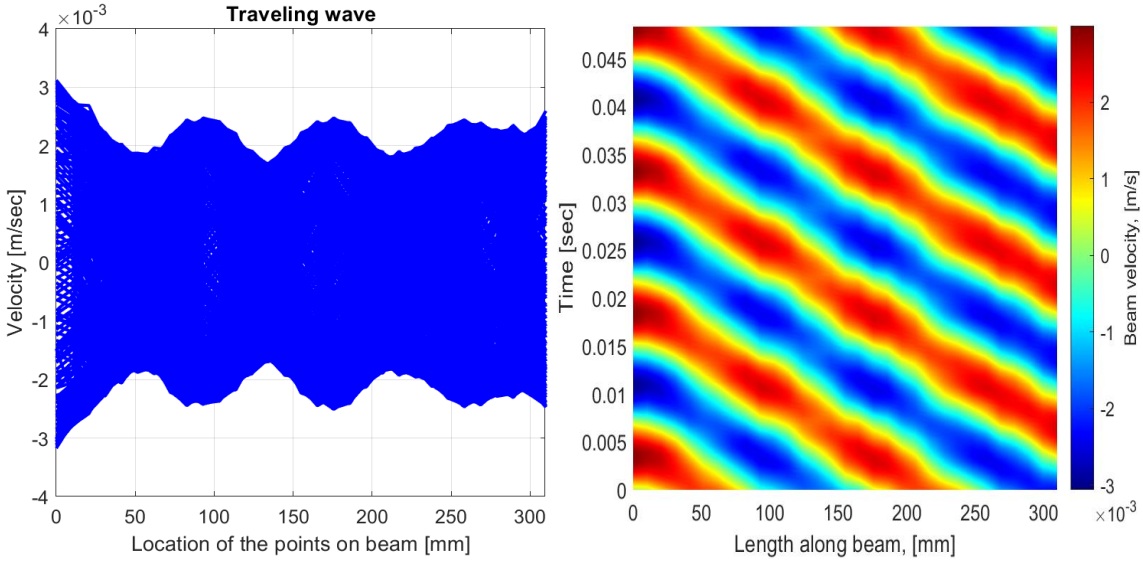

a) Experimental Wave envelop for 67Hz excitation frequency

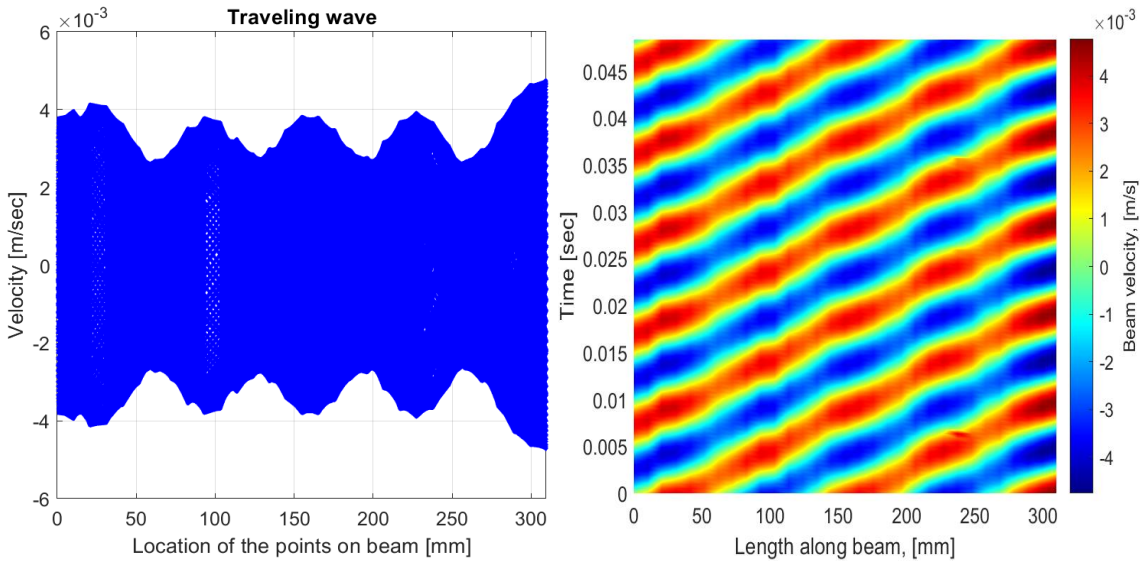

b) Experimental Wave envelop for 104Hz excitation frequency

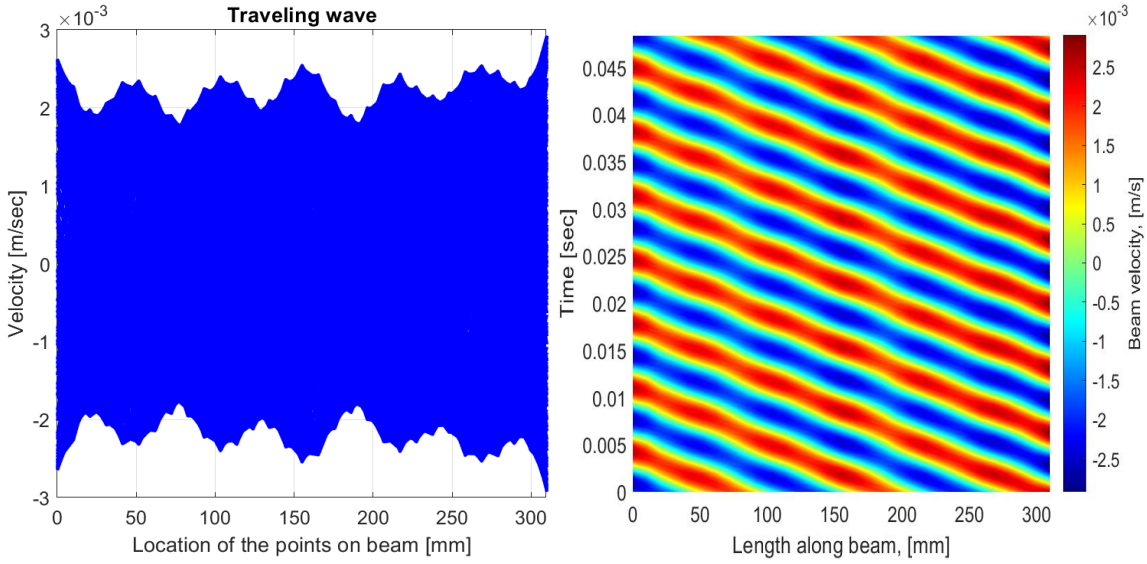

c) Experimental Wave envelop for 147Hz excitation frequency

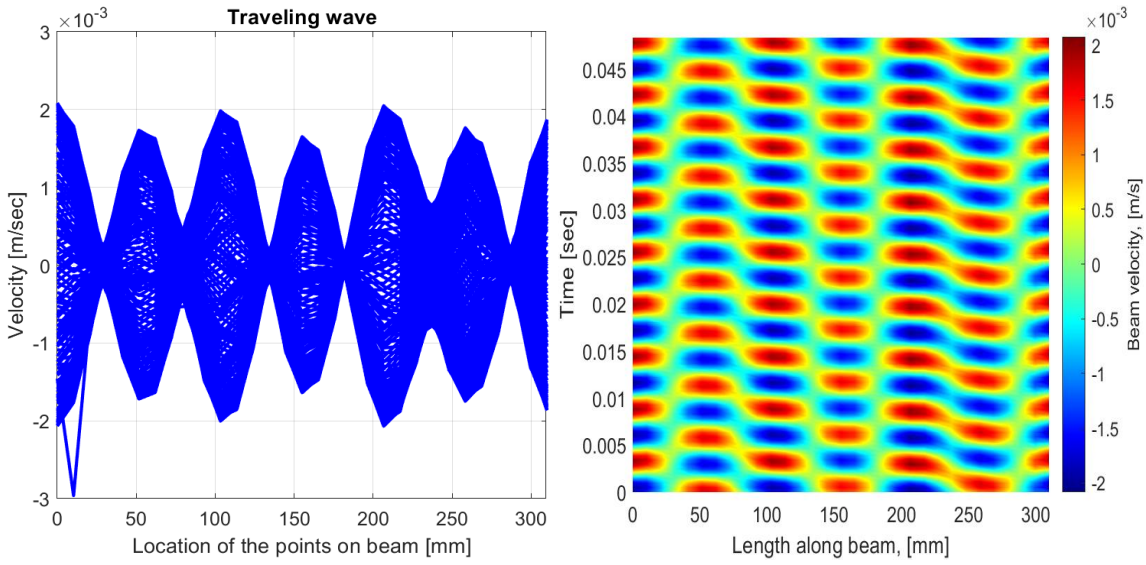

d) Experimental Wave envelop for 179Hz excitation frequency

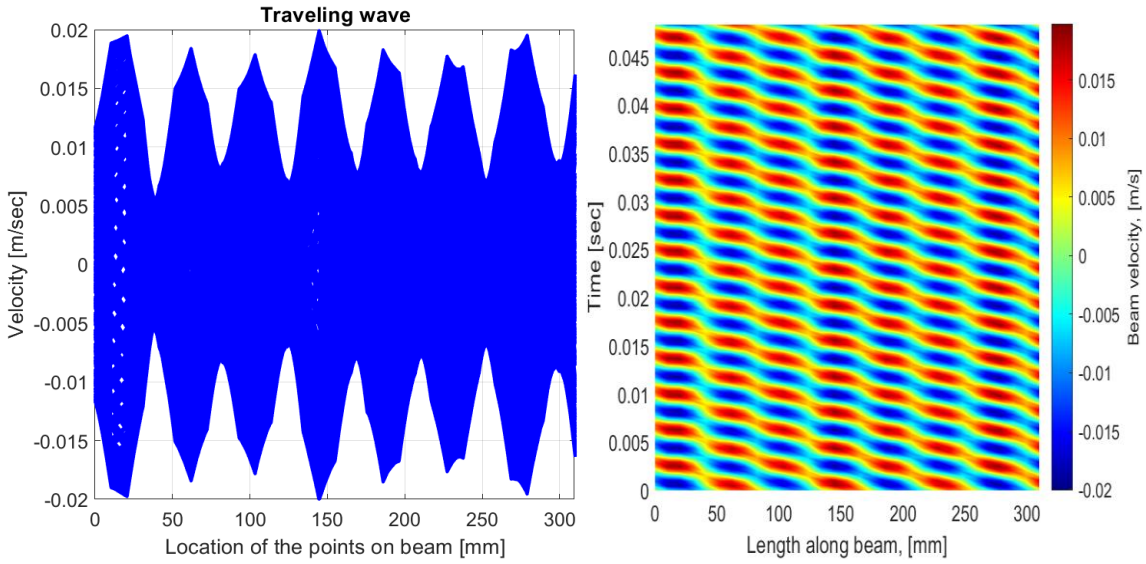

e) Experimental Wave envelop for 270Hz excitation frequency

Figure 3.11: *Experimental velocity wave envelops for generated SBTWs*

Similarly, the wave envelope is plotted for the remaining frequencies used to excite the actuators for generating SBTWs. The table shown below the cost function evaluated from testing data.

Table 3.2: *Experimental Cost function Table*

Frequency	**Experimental Cost Function**
67Hz	0.19
104Hz	0.20
147Hz	0.10
179Hz	0.55
270Hz	0.47

After observing the data in the table, it can be concluded that for 67Hz, 104Hz, and 147Hz the traveling wave component has more weightage that standing wave as the cost function is near to 0. The cost function evaluated from testing are closer to the cost function from simulation. But the wave plot for 179Hz shows some nodal points suggesting it as a standing wave. After carefully observing, the SBTW generated from 179Hz has some parts of traveling wave at start and end and the middle portion is a standing wave.

Same goes for 270Hz, it is a traveling wave, but the standing wave component is dominant. The wave plot for simulation and experimentation are matching.

3.5 Comparison between simulation and testing data

3.5.1 Wave Envelop for 67Hz

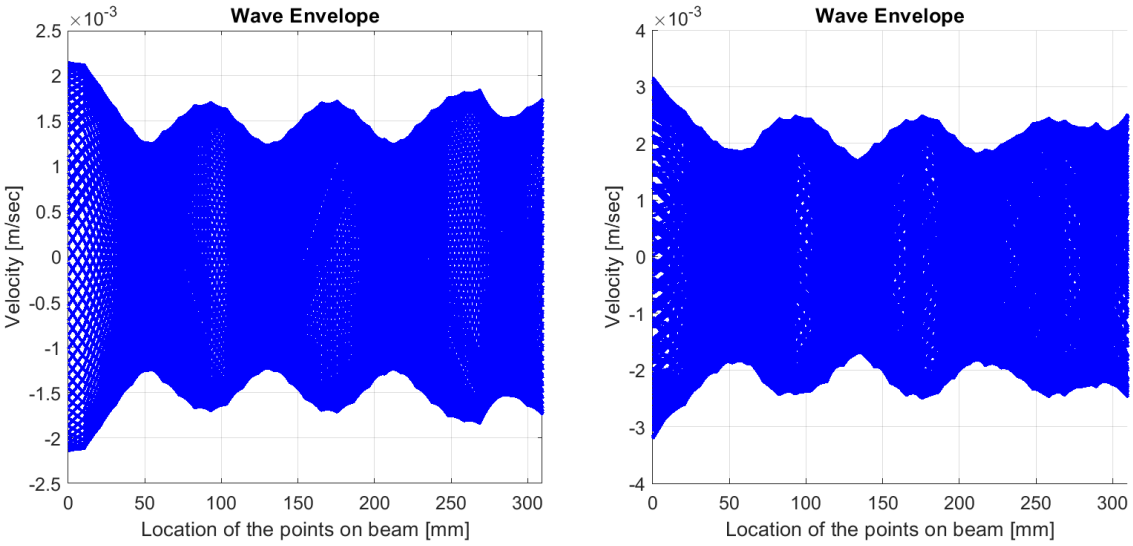

a) Simulation b) Experimental

Figure 3.12: *Wave envelop comparison for 67Hz, Simulation vs Experimental*

Table 3.3: *Cost Function Comparison, 67Hz*

Frequency	**Simulation Cost Function**	**Experimental Cost Function**
67Hz	0.15	0.19

3.5.2 Wave Envelop for 104Hz

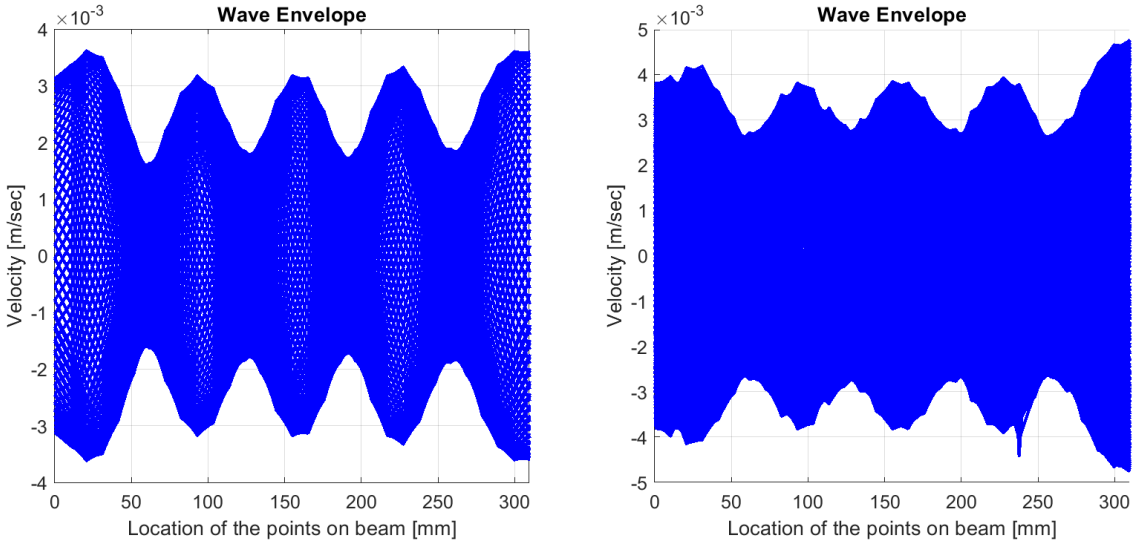

a) Simulation b) Experimental

Figure 3.13: *Wave envelop comparison for 104Hz, Simulation vs Experimental*

Table 3.4: *Cost Function Comparison, 104Hz*

Frequency	**Simulation Cost Function**	**Experimental Cost Function**
104Hz	0.17	0.15

3.5.3 Wave Envelop for 147Hz

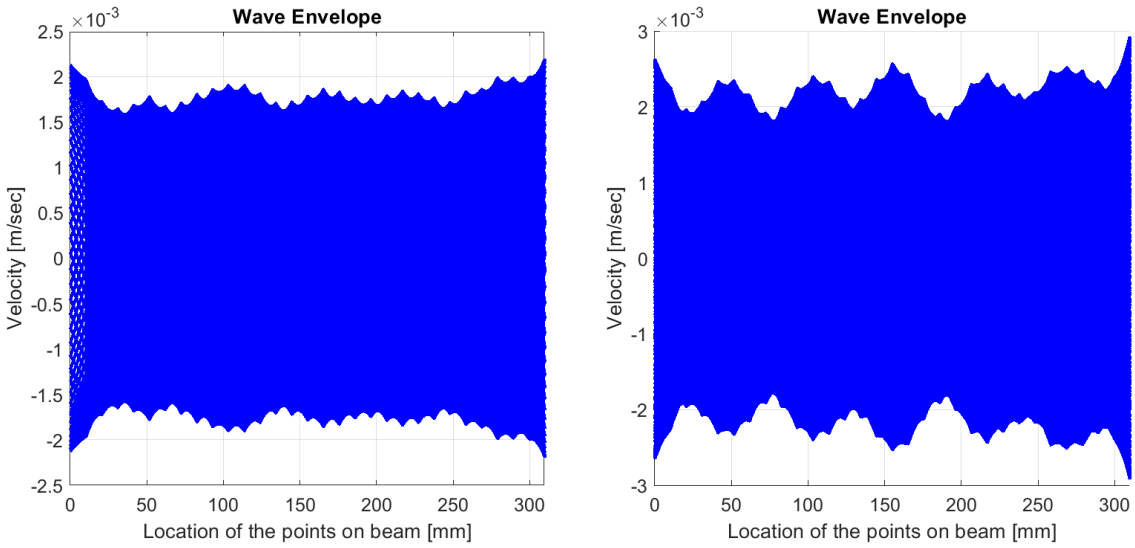

a) Simulation b) Experimental

Figure 3.34: *Wave envelop comparison for 147Hz, Simulation vs Experimental*

Table 3.5: *Cost Function Comparison, 147Hz*

Frequency	**Simulation Cost Function**	**Experimental Cost Function**
147Hz	0.07	0.10

3.5.4 Wave Envelop for 179Hz

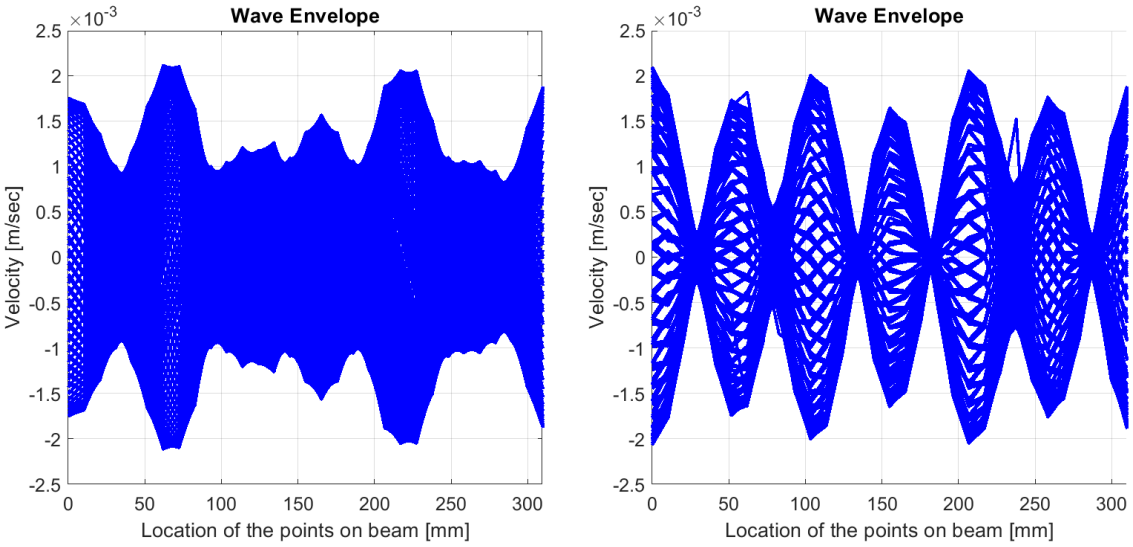

a) Simulation b) Experimental

Figure 3.45: *Wave envelop comparison for 179Hz, Simulation vs Experimental*

Table 3.6: *Cost Function Comparison, 179Hz*

Frequency	**Simulation Cost Function**	**Experimental Cost Function**
179Hz	0.35	0.55

3.5.5 Wave Envelop for 270Hz

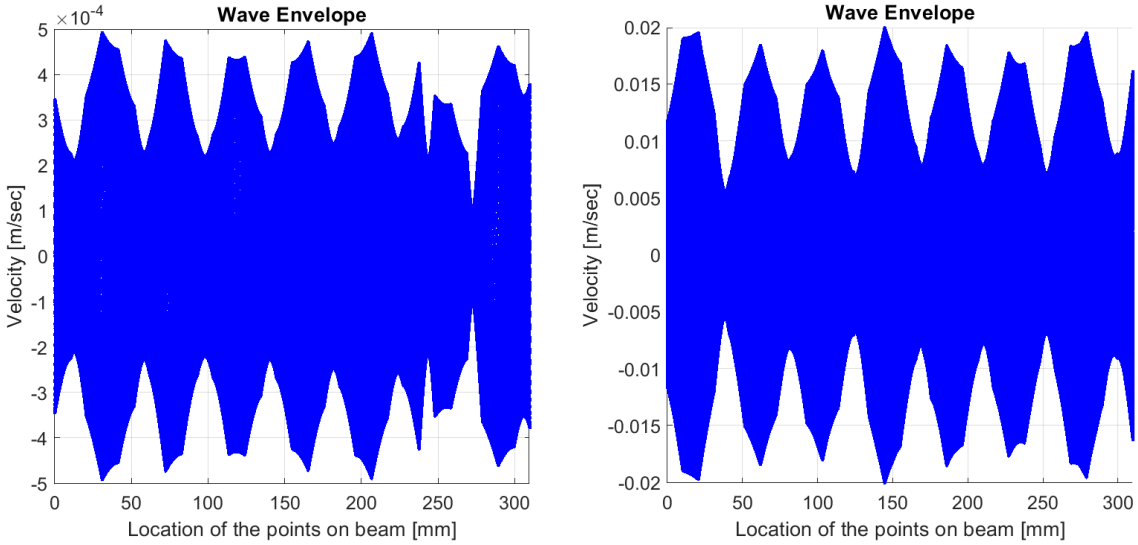

a) Simulation b) Experimental

Figure 3.5: *Wave envelop comparison for 270Hz, Simulation vs Experimental*

Table 3.7: *Cost Function Comparison, 270Hz*

Frequency	**Simulation Cost Function**	**Experimental Cost Function**
270Hz	0.30	0.47

3.6 Guidelines to Tailor Underwater SBTWs

The focus of this chapter was to generate structure borne traveling wave in a simple 1D aluminum beam immersed under water at a depth of 15mm. This chapter follows few steps to generate SBTWs [26] at 5 frequencies depending on different mode shape regions. To summaries this chapter few guidelines are provided below which were followed to tailor successful SBTWs

Step 1: Construct a test setup to perform modal analysis for testing an underwater structure.

Step 2: Perform a modal analysis to acquire natural frequencies and mode shapes. It can be done using an experimental method or numerical method, depending on the complexity of the test structure.

Step 3: Acquire mode shapes and validate them using MAC analysis to ensure the credibility of experimental results. Identify the prospective regions on FRF for SBTWs.

Step 4: Select a middle frequency from two consecutive natural frequencies and use numerical response method to generate wave envelop and validate it using cost function.

Step 5: Use the frequencies selected from numerical simulation for experimental generation of SBTWs. Measure velocities for each point marks on the beam. Plot the RMS values of the velocity against the number of points on the beam to get a wave plot.

Step 6: Compare the wave plots from experimental and numerical method using cost functions to validate the generation of SBTW's experimentally.

3.7 Conclusion

This chapter concluded the successful generation of underwater structure-borne traveling waves in a 1D aluminum beam using two force input method. The focus of this chapter was to prove that SBTW's could be generated underwater. To achieve this, a theoretical model was generated in MATLAB using the data of FRF and mode shapes from the experimental modal analysis. The test setup developed for modal analysis and SBTW generation consisted of two modal shakers attached to a thin aluminum beam that is fully immersed in quiescent water. Data from the modal analysis was used to accurately predict the presence of SBTW at that frequency while optimizing the phase offset and evaluating the cost function.

The second part of this chapter was focused on the experimental study; the frequencies predicted from the MATLAB model were used as excitation frequencies for a sine signal with an offset of 90º. The whole beam was scanned through a laser vibrometer for measuring velocity. The velocity data was then used for validating the cost function acquired from the theoretical model proving that SBTWs were generated underwater.

Chapter 4

Propulsion through SBTWs and Image Processing

4.1 Introduction

In earlier chapter, we learnt about generation of underwater steady state traveling waves using two force input method. This chapter would deal with applying propulsive forces to a 3D printed object on the surface of water through TW generation. So, to move an object a SBTW is generated using the excitation frequencies acquired in earlier chapter with higher voltage range to create undulatory motion in water. An object would be placed over the water surface to show the movement along the direction of wave propagation.

The movement is then recorded using Zed2 stereo camera to understand the velocity attained by the object at different frequencies and varied excitation voltages. Few videos were also captured after changing the direction of wave to show that the direction of propulsion could be controlled using structural dynamics of a wave. These recorded video in post processed using blob analysis to track the motion of the object with respect to time and few observations were made along the way.

4.2 Image Processing

Before generating propulsive forces in water, concepts of image processing need to be discussed. **Figure 4.1** shows the setup for ZED2 camera for recording videos. Location of this camera is very important; it should cover all the area where the object is moving

without any disturbance. Once the camera is installed, the height and the location of camera should be constant. Moreover, the height of water in the tank also should be constant or it would disturb the camera calibration.

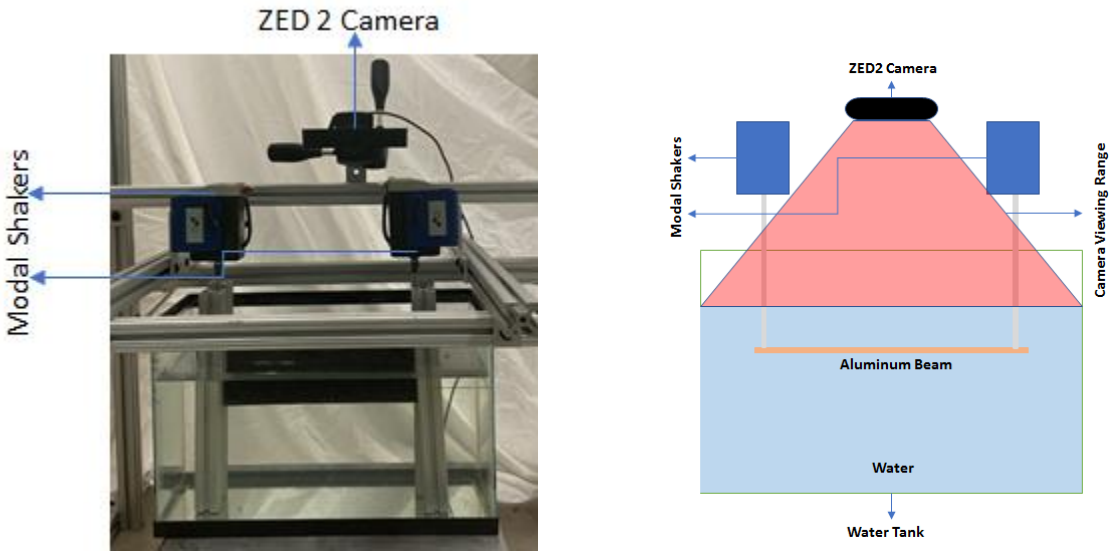

Figure 4.1: *Image processing setup using ZED 2 camera*

4.2.1 Introduction to ZED 2 stereo camera

Figure 4.2: *ZED 2 Stereo camera image*

Figure 4.2 shows the ZED 2 camera which is an updated version of ZED camera developed by STEREOLABS for HD 3D video recording with neural depth sensors to gauge the environment [27]. This camera has been designed for challenging applications

such as spatial object tracking, autonomous navigation and mapping to augmented reality. This updated version has a better viewing angle of 120° width and an improved positional tracking. It is also equipped with cloud connect technology where this camera could be controlled remotely. The neural depth sensors help this camera to track the object, map the surroundings, measure height and orientation of floors and could also be used to detect human body skeletons.

As the research required tracking the motion of an object moving over the surface of water, this camera was the best choice for it. This camera was used for recording 1080p videos at 30fps. The outputs acquired from object detection and motion tracking functions were bounding boxes for 3D/2D shapes, location, speed, and segmentation masks.

4.2.2 Camera Calibration

Before recording any videos for image processing, it is necessary to calibrate the camera to acquire the camera properties such as focal length, rotational matrix and principal point matrix. These values are very useful in image processing to create a coordinate system. To calibrate ZED2 camera a checkerboard was printed with a size of 11 × 8 checkers with 15mm length. The checkerboard is shown in **Figure 4.3**. The checkerboard images are used in camera calibrator app where the app identifies all the corners of each checker and tries to compute re-projection errors by projecting the points on the checkerboard using world coordinates. The projected points are then compared to detected point for error evaluation [28].

Few steps are given below on how calibrate a camera in MATLAB.

Figure 4.3: *Checkerboard Calibration of Zed2 camera at water level to acquire camera intrinsic*

Step 1: Place the checkerboard on the water surface and move it manually covering all the area of the water tank. While doing this, record the video from the camera which needs to be calibrated. Disintegrate the video to acquire images. For this research 120 images were used to calibrate the camera.

Step 2: Open the camera calibrator app from MATLAB and insert all the images while entering the length of single checker to convert pixel coordinate system to world coordinate system. The calibrator app would detect the points on the checkerboard for all the images. **Figure 4.3** shows an example of a checkerboard with detected points.

Figure 4.4: *Camera Calibration image after re-projection of checkerboard points*

Step 3*:* After uploading images, calibrate the camera. This would project points on the checkerboard and compare it with detected points while calculating errors. **Figure 4.4** shows re-projected points over the board with + symbol. Check for mean calibration error and delete outlier images if needed. **Figure 4.5** shows the plot for re-projection error for all 120 images. The mean error is just 0.16 pixels.

Step 4: If required, update the model by recapturing all the images with checkerboard and repeat step 1 – 3 to get better results.

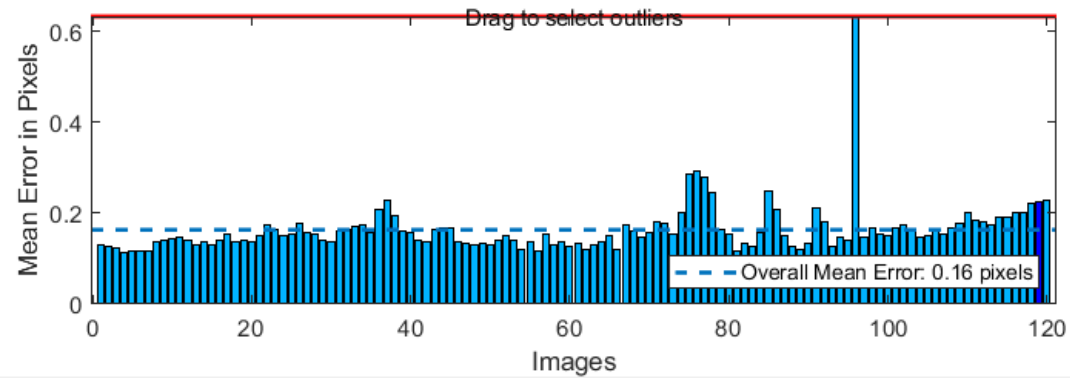

Figure 4.5: *Mean Image Calibration error in pixels after the calibration*

4.2.3 Blob Analysis using Kalman Filter

Blob analysis is the most basic method to binarize an image for a particular area in an image known as a lump/blob to analyze its features such as shape, area, position, length and direction of the blob. After the video is recorded from ZED2 camera, an image is selected from it. This image is then uploaded in Color Threshold app where the object's color is isolated creating a greyscale image which only has values of 0 and 1. This method is known as masking. In the blob analysis a bounding box is created around the lump having 1 as the binary value and is traced frame by frame while evaluating the pixel coordinates of the blob with respect to time.

While performing blob analysis undesired noise in the data of coordinate system could be induced so, to avoid that the Kalman filter is used for probabilistic analysis to predict the desired motion of the blob. Kalman filter follows the trend from blob analysis and predict the motion when there is uncertainty in the data. The world coordinate system is applied on the conditioned data from Kalman filter to evaluate the speed and distance of the blob in real time. This research uses a 3D printed thin square object of orange color with the

dimensions of 20mm × 20mm × 1mm. The object is made of Polylactic Acid (PLA). The predefined dimensions of this object/blob are used to validate the data from blob analysis. The dimensions of the object are the predicted using bounding box and are compared with the real dimensions for validation.

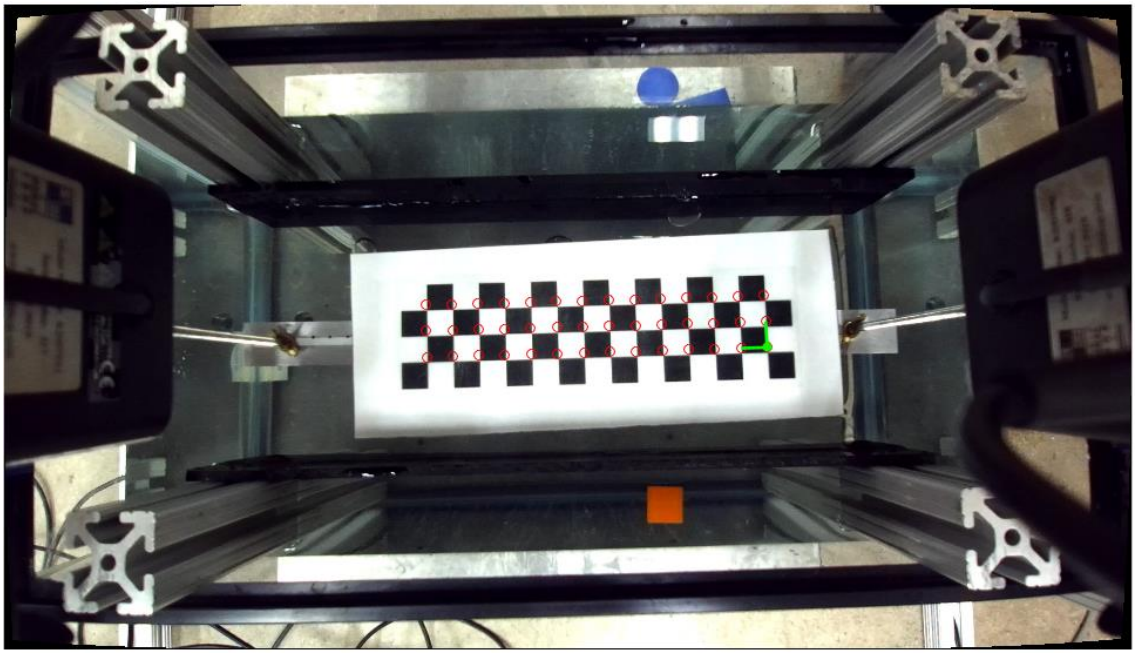

Figure 4 6: *Calibration checkerboard to set an origin for the world coordinates*

4.3 Analysis on object's movement influenced by SBTWs

To generate traveling wave in beam immersed underwater, the shakers were simultaneously excited with a sinusoidal signal and a phase offset of 90º between them. This section generates 5 SBTWs at the frequencies of 67Hz, 104Hz, 147Hz, 179Hz, and 270Hz. For each frequency the object is shown moving, and 5 videos are recorded to show the average motion. For each video, blob analysis is performed showing the motion

of object in pixel coordinate system and world coordinate system. The displacement and velocity with respect to time are also plotted.

The **Figure 4.7** shows the snapshots of object's motion over the surface of water influenced by traveling waves at different interval of time. It could be clearly observed that the orange object is moving in left direction along the water channel.

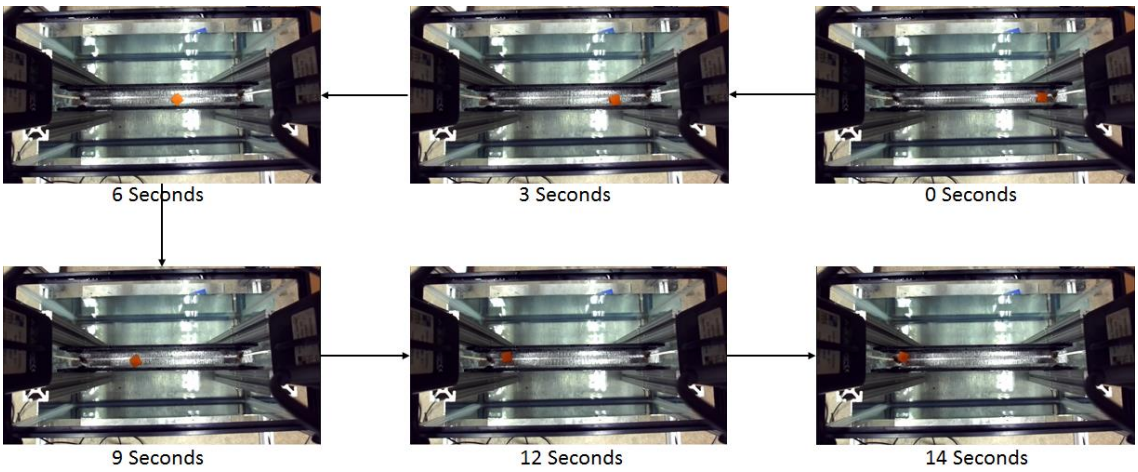

Figure 4.7: *Object's motion snapshots for 67Hz TW frequency*

Figure 4.8 displays the output for blob analysis with a group of plots holding the information of velocity, displacement and time of the traced object. The first plot shows the object's initial location and the path traveled by it for 5 videos. The bottom left plot shows the y position and x position traveled by the object in millimeter. In this case the average distance traveled by this blob is 290mm.

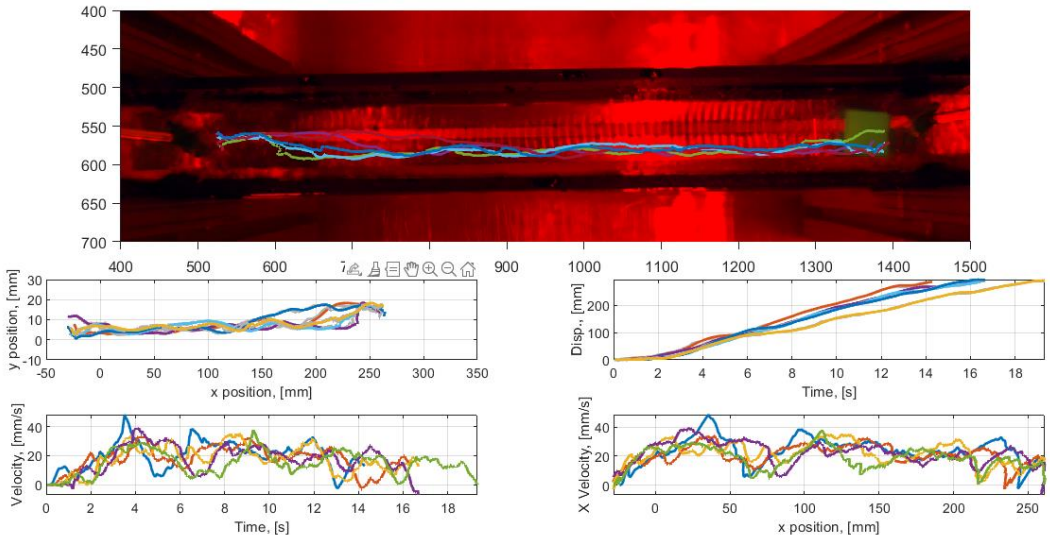

Figure 4.8: *Image processing plot using Blob analysis at 67Hz for 5 videos*

The right-side plot shows the displacement (mm) of the object with respect to the time. The longest time taken for this object to travel the given distance is 18 sec. The remaining plots show the instantaneous velocity with respect to time and x-position. The blob attained a top speed of 40mm/sec at 67Hz excitation frequency.

For the above case, while exciting the aluminum beam with two shakers the phase offset between their signals was chosen to be 90º. The direction of motion of the object was from right to left. So, to check the effect of phase angle to the direction of motion, the phase offset was changed to -90º and then the shakers were excited for 67Hz and two videos were recorded. The **Figure 4.8** shows the change in direction of the object's motion. At first the object was moving from right to left and in this case, it could be clearly observed that the direction has reversed. So, this concludes that in this propulsion system the object could be maneuvered using appropriate phase offset.

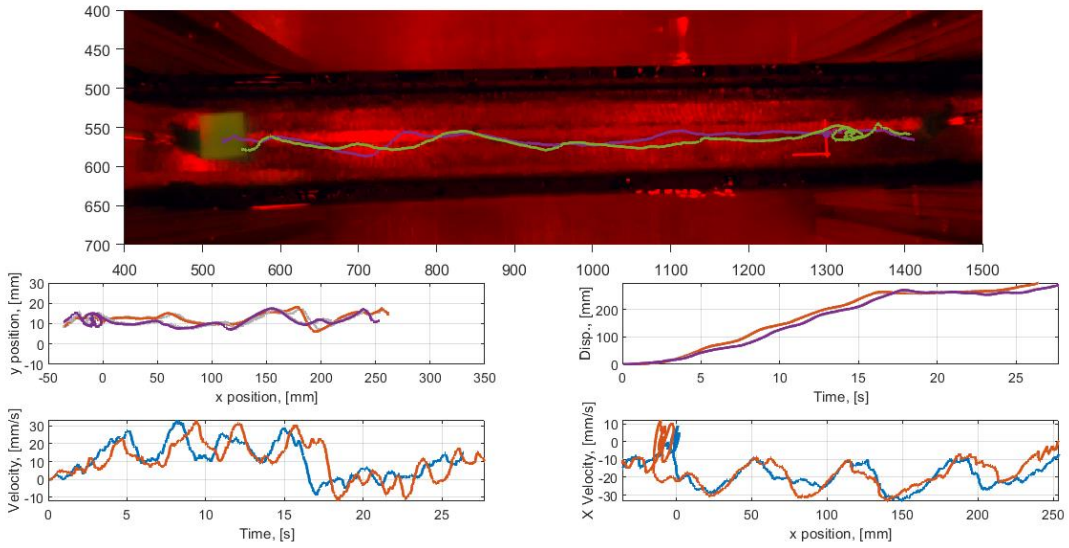

Figure 4.9 *Blob analysis for -90º phase offset at 67Hz*

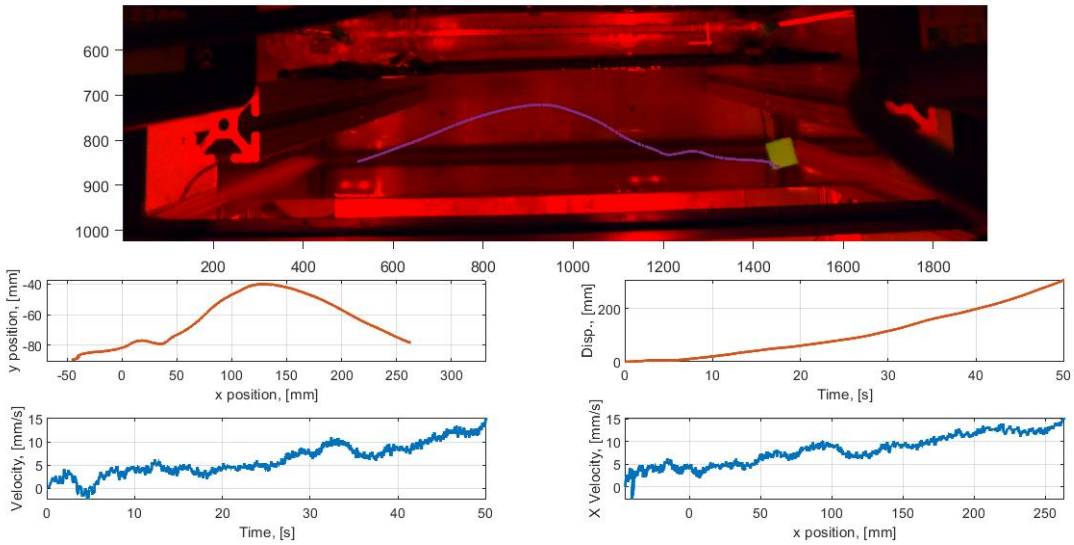

Figure 4.10: *The motion of the object shown outside the water channel*

As the research progressed, a question arose that is the water flowing due to the influence of traveling wave or just showing wave like patterns. So, to answer this question the SBTWs were created at 67Hz with -90º phase offset and now the object was placed

outside of the water channel. So, in **Figure 4.9** it was observed that after the SBTW starts and the water starts showing wave inside the channel, the object placed outside the channel also starts moving but in the opposite direction of the wave. This shows that the water actually moves with the wave creating two vortices in the tank. The water starts moving inside the channel from left side and splits in two ways at the end of the channel creating two vortices. So, if a object is placed outside, at the end of the channel then it returns to the initiation point of the flow.

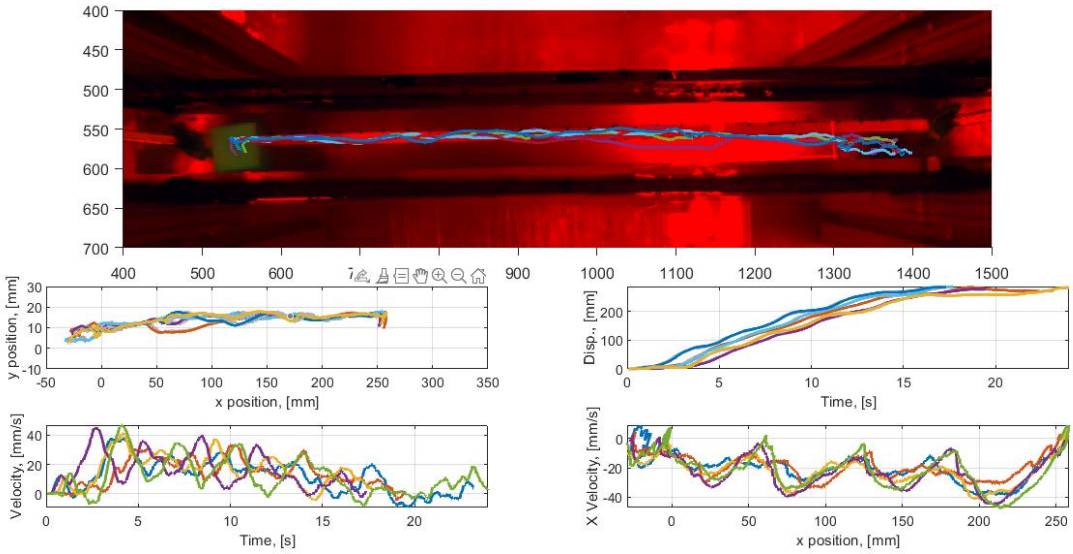

Figure 4.11: *Image processing plot using Blob analysis at 104Hz for 5 videos*

The same process of generating SBTWs by exciting shaker to record the videos of an object moving over the surface of water was carried out at 104Hz excitation frequency. In this case if we observe the x-velocity vs x-position plot, we could see three humps in the x-velocity which resembles the wave envelop for 104Hz shown in chapter 3. So, there

might be a chance that the velocity is dependent on the wave amplitude of excitation frequency.

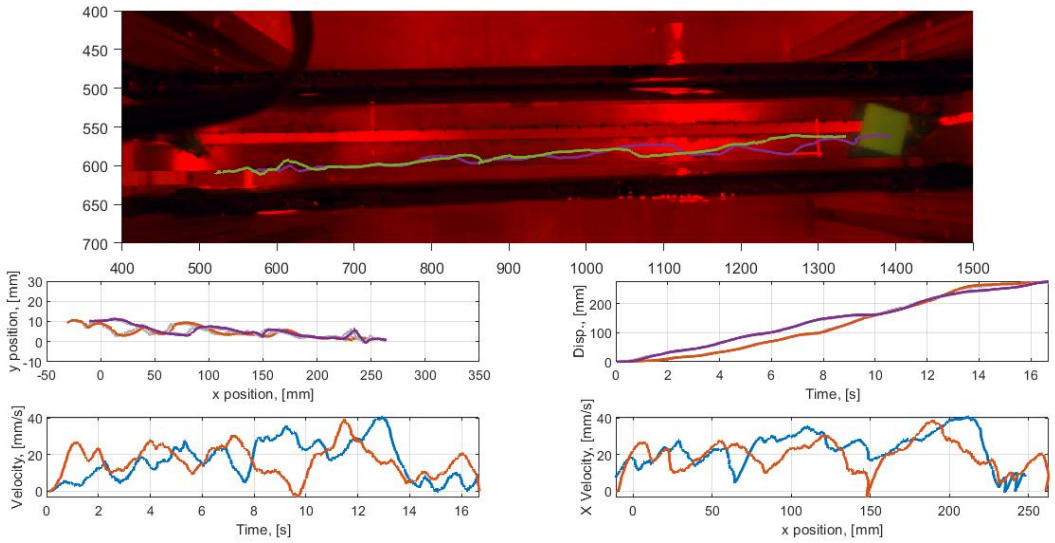

Figure 4.12: *Blob analysis for -90º phase offset at 104Hz*

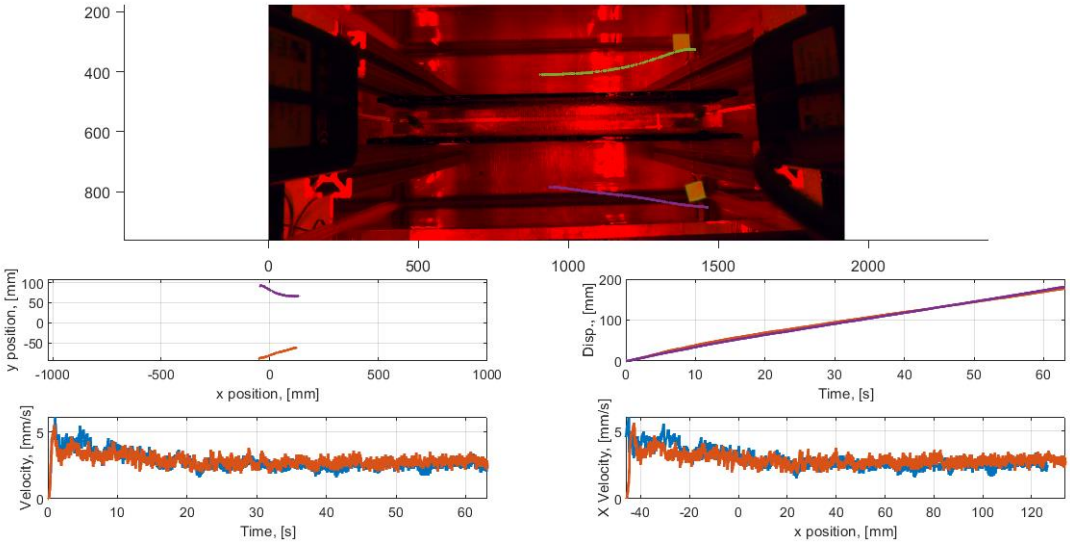

Figure 4.13: *The motion of the object shown outside the water channel for 104Hz*

The videos with negative phase angle and object placed outside the rails were also recorded to check if the direction change and water vortices are not just depended on 67Hz frequency. So, after performing image processing the theory for direction change and water vortices check out for 104Hz as well.

All these processes were carried out for the rest of frequencies as well. Below are the figures which shows the image processing plots for 147Hz, 179Hz and 270Hz

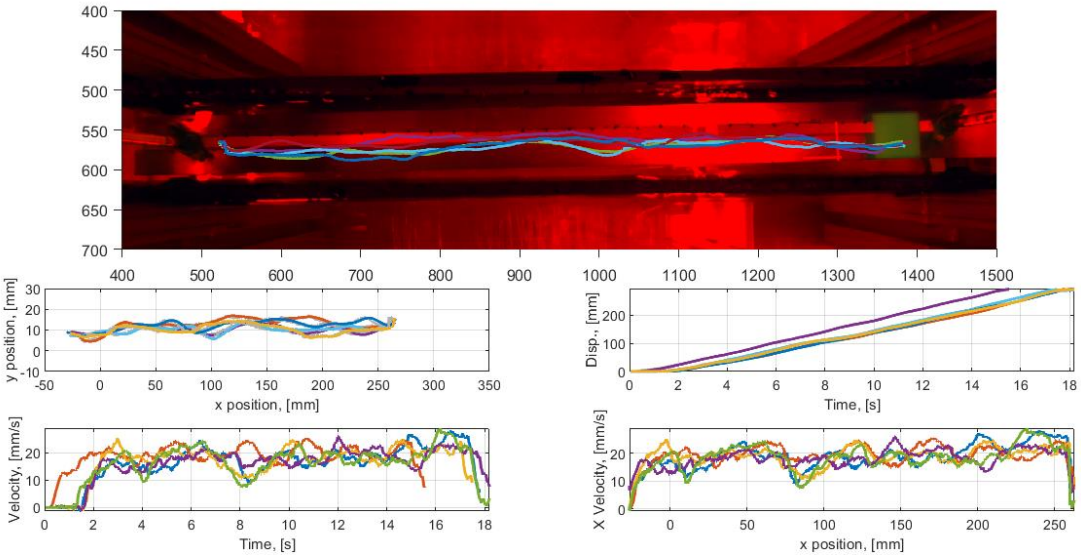

Figure 4.14: *Image processing plot using Blob analysis at 147Hz for 5 videos*

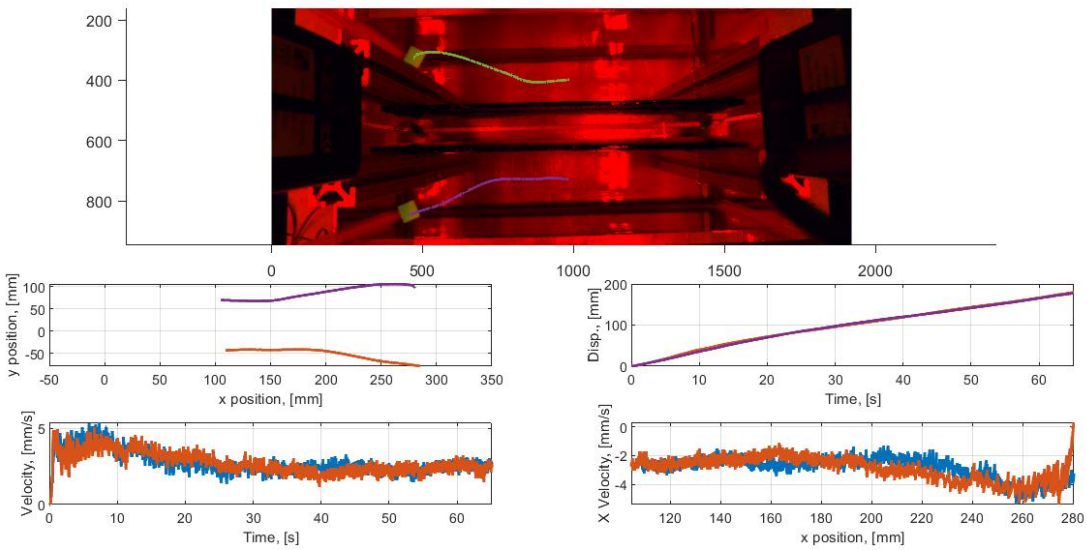

Figure 4.15: *The motion of the object shown outside the water channel for 147Hz*

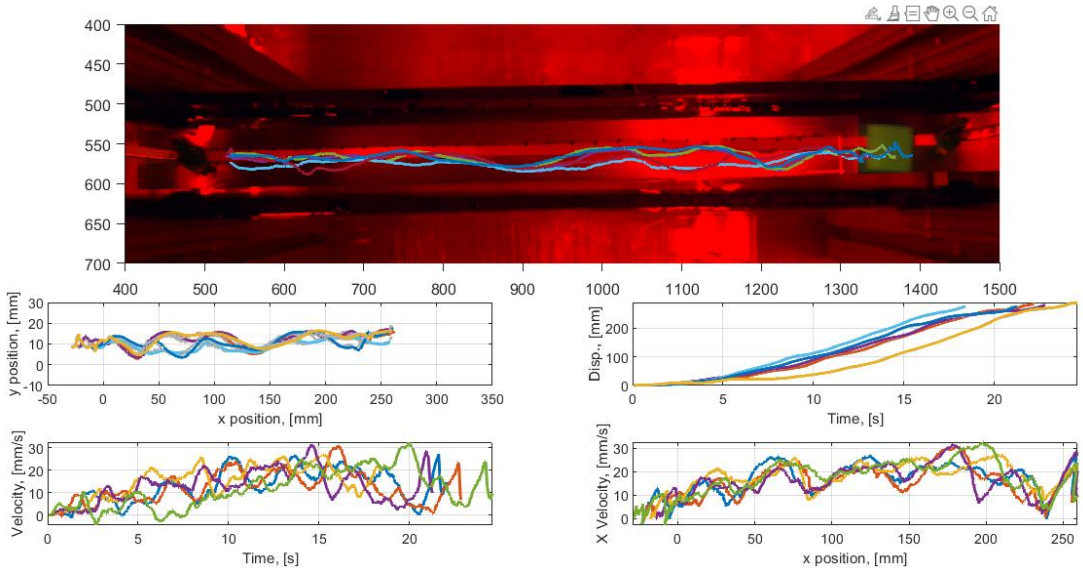

Figure 4.16: *Image processing plot using Blob analysis at 179Hz for 5 videos*

As it is known from chapter 3 that SBTW generated at 179Hz has dominance from standing wave component. But here we can still see the object moving while attaining an average velocity of 24mm/sec. This could happen because of the traveling wave

component which is still present in that wave. The TW component might be giving the necessary thrust to move the object along with the water.

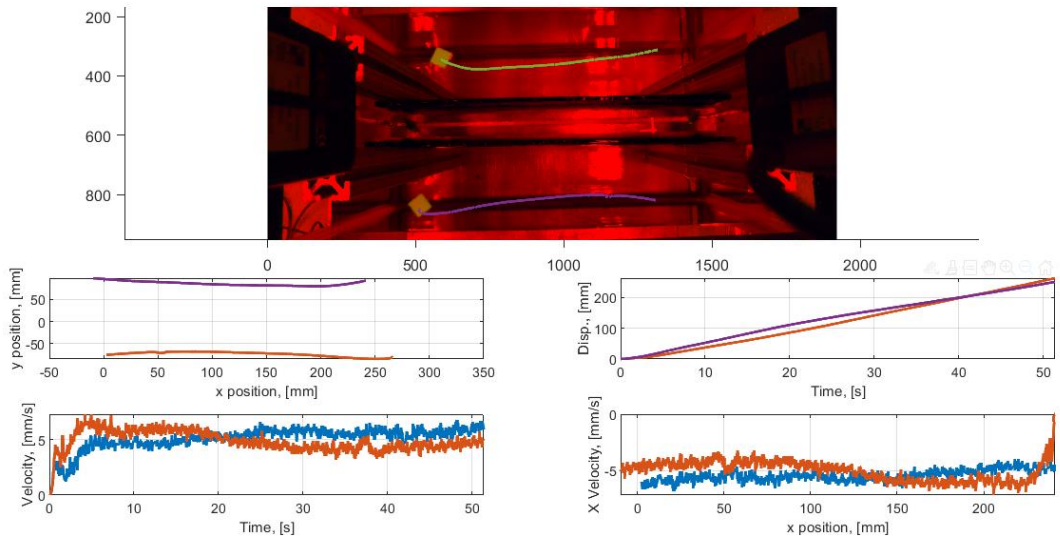

Figure 4.17: *The motion of the object shown outside the water channel for 179Hz*

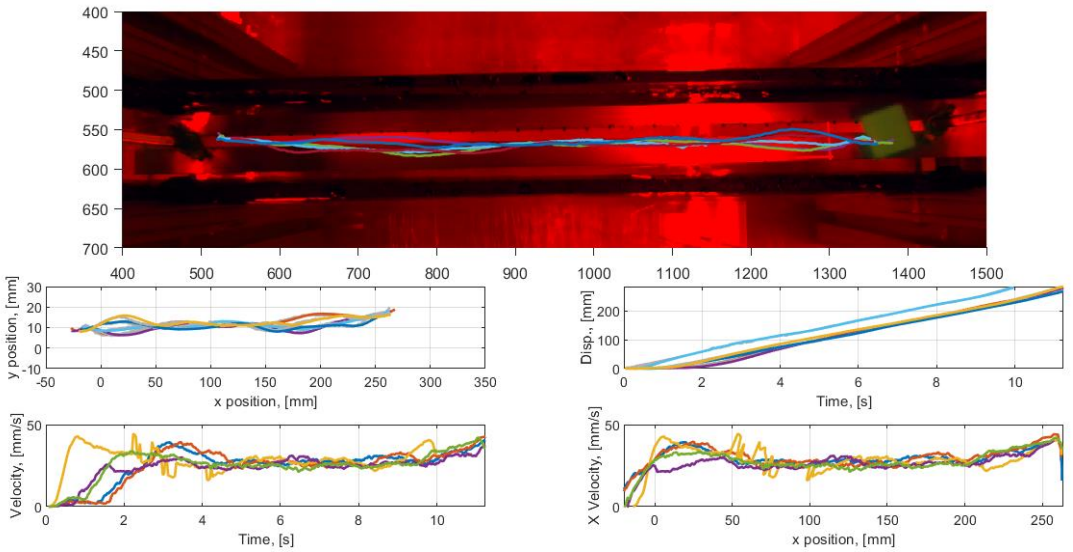

Figure 4.18: *Image processing plot using Blob analysis at 270Hz for 5 videos*

4.4 Voltage dependent wave velocity

In this experimental study we wanted to know more about the SBTW's behavior and how it is dependent on the excitation voltage. So, to study this 104Hz and 147Hz frequency SBTWs were selected as they are more stable waves with a low-cost function than others.

First the 104Hz frequency was used to excite the shakers with 0.7V. The motion of the object was recorded and then this step was repeated using 0.1V and 0.13V. These voltages were selected such that it should be enough to provide a thrust to the object for its motion and it should be in a range where the flow of the water is not disturbed due to high amplitude.

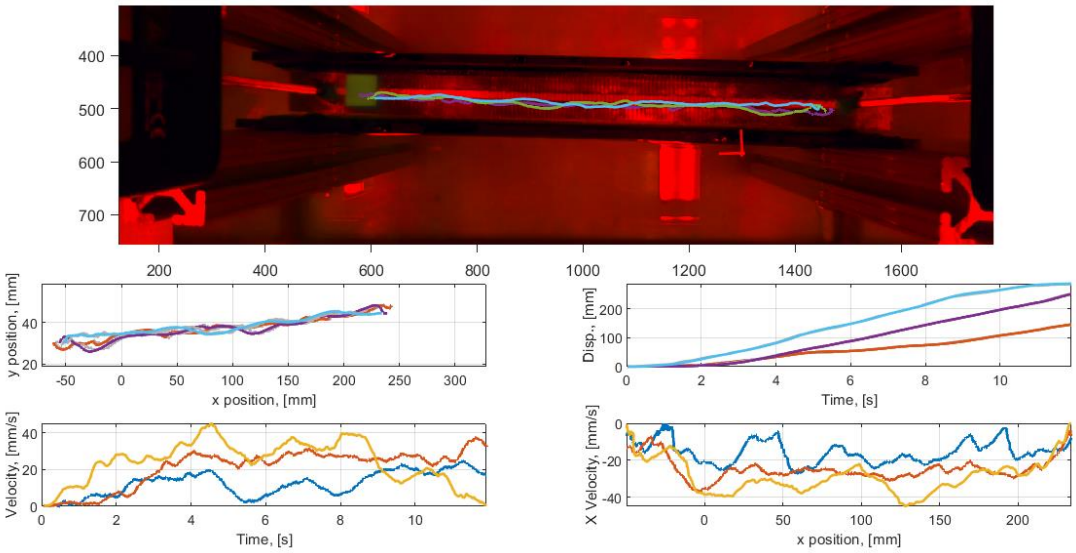

Figure 4.19: *Image processing plot comparing the velocities of the object at 3 different voltages for 104Hz*

So, it could be observed from the velocity vs time plot that as we are increasing the voltage, we could also observe a slight increase in the velocity of the object too. To

confirm this hypothesis the beam was once again excited using 147Hz with 0.1V, 0.15V and 0.2V. The videos were recorded and image processing was carried out to plot the velocity vs time graph.

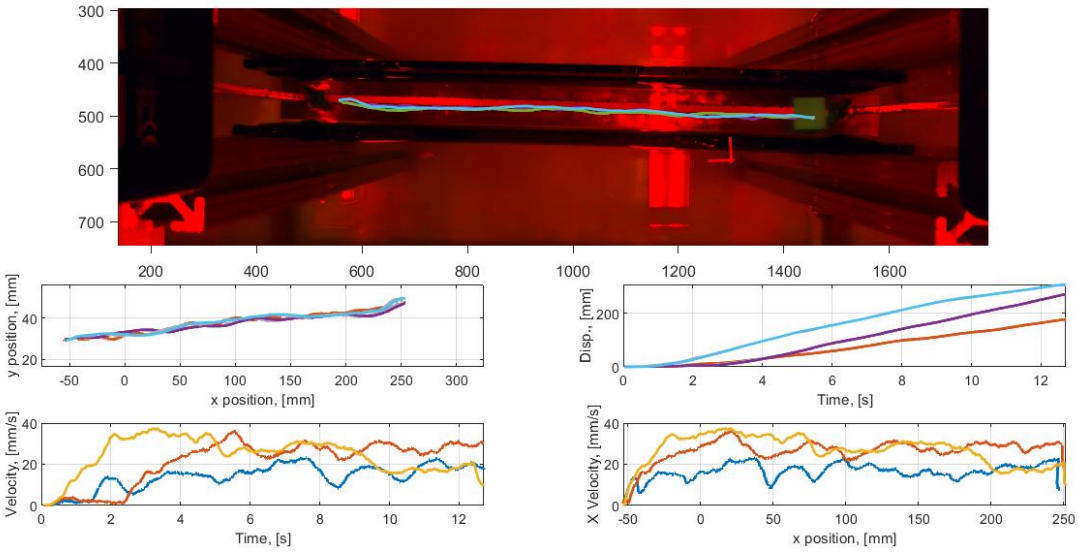

Figure 4.20: *Image processing plot comparing the velocities of the object at 3 different voltages for 147Hz*

Figure 4.17 shows the results of image processing for 3 videos with varied voltage. In this case the initial velocities of the object are increasing with the voltage. But the velocities are varying excessively. This makes it difficult to conclude that if the excitation voltage is increased, the velocity of the object also increases.

So, to strengthen this argument, a test was performed where all five excitation frequencies were selected. A varying voltage range was selected for each frequency according to their resonating force for that particular mode shape. The beam was divided into 31 points, so 15th point was selected and the SLDV was pointed towards it.

Shakers were excited with 67Hz frequency at 0.01V, 0.025V, 0.05V, 0.075V and 0.1V. The velocity response at that point was measured by the laser. This process was carried out for the rest of the frequencies with different voltage ranges and the data was converted to a MATLAB file.

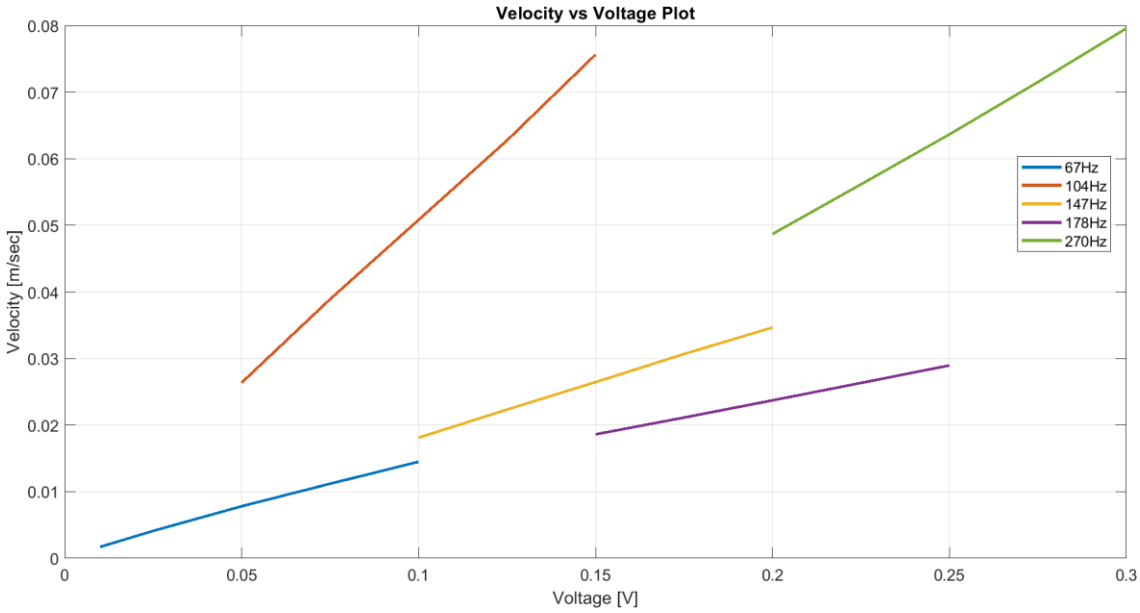

Figure 4.21: *RMS velocity vs voltage plot showing all 5 frequencies*

The **Figure 4.18** clearly has shown the linear increase in the velocity as the voltage is increased. And this is true for all the frequencies we tested. So, this plot confirms our hypothesis that the wave velocity is affected by the excitation voltage. The initial theory was shown through image processing and to validate this theory laser vibrometer was used as it gives more accurate data than that of image processing.

4.5 Wave velocity of traveling wave generated in aluminum beam

Till now this paper only discussed the object velocity and beam's point velocity. But, a curious mind wanted to find the velocity generated by traveling wave in the water which was a driving force for the object's motion. So to find the wave velocity, single point laser vibromter was used to acquire special point velocities for 31 points which were marked on the beam. The beam was excited by the shakers with all the traveling wave frequencies which have been mentioned in chapter 3. The figure 4.22 below shows a plot of a peak from the 31 points of velocity tracked with respect of time throughout the beam length. And a zoomed in color map of 67Hz's traveling wave.

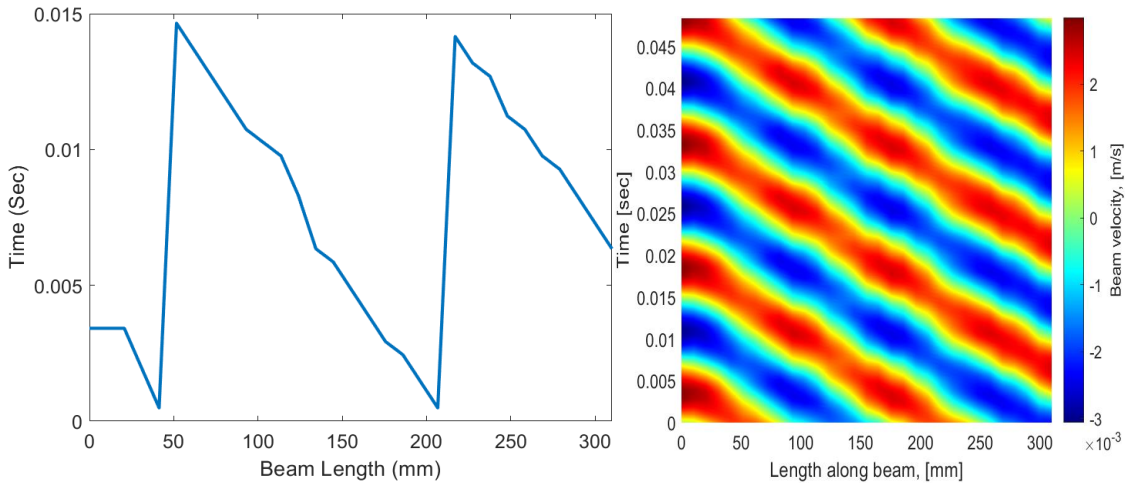

Figure 4.22: *Plot for point tracked throughout the beam length with respect to time*

The idea was to track a point on the beam till it reaches the end of beam, through which time can be obtained for a point to cover the length of a beam. And if you have time and distance then you can get average velocity of a wave. So, with this idea a MATLAB code was generated to calculate wave velocities for all the waves which are mentioned in the

Table 4.1**.** As the laser was positioned at the top of the beam while recording data, we could only get the data in Z direction and the velocities which are mentioned below are in Z direction and cannot be compared with the object's velocity obtained in image processing.

Table 4.1: *Wave velocity values for all the traveling waves*

Frequecy (Hz)	**Wave Velocity (mm/s)**
67	3.79E+03
104	1.39E+04
147	2.40E+03
179	3.28E+04
270	1.24E+03

4.6 Correlation between Object velocity and Beam velocity

After calculating wave velocities, we analyzed the data to draw a relation between the object's velocity envelope trend and beam's velocity envelope trend obtained from image processing and laser vibrometer respectively. But to do this it was necessary that there should be no offset between the beam and object velocity envelop so that they can overlap on each other in a plot. An offset factor was calculated using the data from image processing with a value of 42.599mm. This value was subtracted from the location vector

of beam's velocity. The **Figure 4.23** shows all the velocity data obtained for 103Hz TW from image processing and laser vibrometer overlapped on each other.

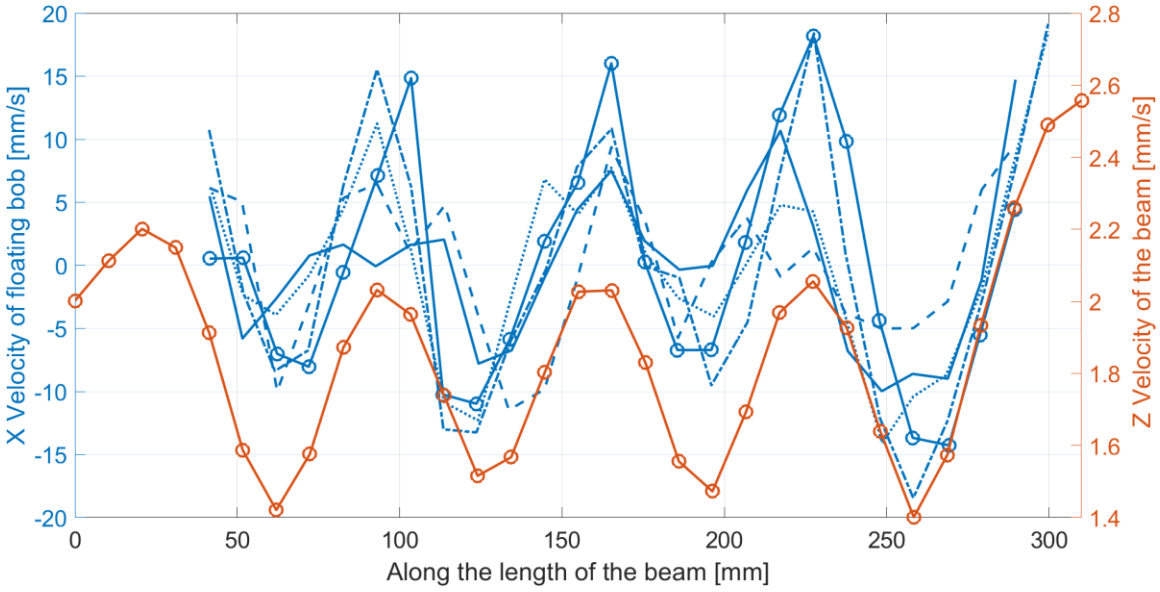

Figure 4.23: *Plot showing overlapped velocity of beam and object velocity*

It could be observed that the trend followed by the beam velocity matches with the object's velocity i.e. when the beam velocity is at maximum then the object velocity is at maximum too. To further comment on this trend, the correlation was calculated for all the TW frequencies. The best correlation was observed for 103Hz with 0 lags. The values for correlation and lags are mention in the **Table 4.2.**

Further study needs to be performed in this area to know more about the effects of travelling wave on objects motion.

Table 4.2: *Correlation and lag values between the object's velocity and beam velocity*

	TW_64Hz		**TW_103Hz**		**TW_147Hz**		**TW_179Hz**		**TW_270Hz**	
	Max Correlation	Lags	Max Correlation	Lags	Max Correlation	Lags	Max Correlation	Lags	Max Correlation	Lags
1	0.5704	62.02	0.6995	0	0.3777	103.2667	0.5608	0	0.2332	-41.4143
2	0.4691	-82.4	0.6294	0	0.6803	-30.9815	0.4269	0	0.1837	10.3371
3	0.6917	-72.2	0.8385	0	0.537	31.08122	0.5494	0	0.3127	93.09469
4	0.385	-41.3	0.9023	0	0.3868	-61.8267	0.4423	0	0.3297	-10.3199
5	0.7746	-20.6	0.7946	0	0.4459	61.94517	0.2851	-62.0228	0.2221	-30.9045

4.7 Conclusion

This chapter focused on generating propulsive forces underwater through tailoring high-quality structure borne traveling waves in the aluminum beam. Using the data from previous chapter a steady state traveling wave was generated selecting appropriate excitation voltage which could provide desired thrust for the object's motion. By

achieving the object's motion influenced by SBTW this experimental study successfully established that SBTWs are capable for moving an object over the surface of water. The recorded videos of the object were used for image processing to study the effect of SBTW frequencies on the velocity. In this section controlling the direction of motion or wave was achieved through changing the phase angle to -90º.

The later part of this chapter discussed the effects of voltage over the object's velocity through image processing and then it was validated through measuring the wave velocity with SLDV. It was concluded that the velocity is directly proportional to the applied excitation voltage. Further analysis between the beam velocity and object's velocity was done and an observation was drawn about their trend similarity.

Chapter 5

Conclusions and future work

5.1 Conclusions

This experimental study was based on the concept that traveling waves could be generated in a finite structure and the waves have propulsive effects. To prove this, a setup was constructed for experimental modal analysis which is explained in chapter 2. The aluminum beam was immersed under water using pined-pined boundary conditions. Using shaker excitation method, mode shapes and natural frequencies of the structure were obtained. The test results were successfully validated using modal assurance chart analysis were the correlation between experimental and simulated mode shapes was very high.

The data collected from modal analysis was used to find potential frequency regions to generate the structure borne traveling waves. The TW generated in discussed in chapter 3 in detail. Five regions were found with consecutive natural frequencies and the middle frequency of each region was chosen. A numerical model was used to simulate the response for two single-point force excitations method. The response from numerical method showed wave envelops for 5 SBTW frequencies with their cost function values. The cost functions were positively validated with the experimental wave envelops and their cost functions. This chapter concluded with successful generation of underwater structure borne traveling waves in an aluminum beam.

Chapter 4 concluded the propulsive forces present in the structure borne traveling waves. After the SBTWs were generated, it created two vortices in water which were channeled by the directional rails placed inside the water tank. A 3D printed square shaped object was placed on the surface of water which propelled along the motion of the water while the SBTWs are generated in the beam. The motion of the object was recorded using ZED2 stereo camera to trace the displacement of the object. Through image processing and blob analysis, velocity of the object's motion was calculated for each frequency. The object achieved max velocity of 40mm/sec. While testing the direction of motion of the wave, it was concluded that the object could be maneuvered using phase offset between the signals of two actuators. It was observed that as the phase offset was changed to -90º, the direction of wave was reversed and which in turn reversed the direction of the object.

After observing the x-position velocity plot for 104Hz and comparing it with the experimental wave envelop, it was concluded that there might me some relationship between the wave's particle velocity and object velocity as both were following identical trends. Another observation was made on the relationship between the excitation voltage and the velocity gained by the object. Varied voltage input was given to the shakers for 104Hz and 147Hz frequencies and the motion of the object was recorded. The videos were analyzed for the instantaneous velocities and a trend of increase in the velocity was observed when voltage was increased. To confirm this hypothesis, velocities at a fixed location were measured for the 5 SBTW frequencies by laser vibrometer at increasing voltages. The data was plotted as velocity vs voltage. A linear increase in the velocity

was observed with respect to the voltage confirming that velocity of the object is directly proportional to the excitation voltage.

The research successfully concluded that SBTWs could be used for underwater propulsion system, but still a lot more research needs to be performed in order to use this method as an alternative for conventional multi actuator-based propulsion system. The next section discusses the future work that could be done on this research to improve the results.

5.2 Future Work

This study only proved the potential of SBTWs towards the underwater propulsive forces. A further research needs to be done to know the reason of the water flow and the vortices created by the SBTW. The thrust calculation is also needed if this method is to be used as propulsion system for aquatic robots.

The two-point force input method was used to generate SBTWs in this experimental study where two actuators where used. To reduce the number of actuator and simplify the process of SBTW generation, a study on using a single actuator for tailoring traveling waves should be performed. This would reduce the energy consumption and complexity of the setup. Some preliminary studies were performed on this method where single shaker to excite the aluminum beam is used along with three dashpot dampers.

5.2.1 Preliminary experimental study for SBTW generation using single point force method

The idea behind this experiment was to check if the dashpot dampers act as single point force input creating a phase difference between shaker output and its own force input to the beam. If the dampers could act like this then it would be possible to generate traveling waves in a structure using just one excitation input. Some simulations were performed to check if the response of single force input with a system of spring-damper produces a TW. With these simulations it was proved that, it is possible to generate a TW using this system as we achieved a cost function of 0.058 at a frequency of 1459.6Hz.

Further it was thought that, it could also be possible to use multiple spring-damper systems to generate multiple traveling waves at different locations with different frequencies. This would help in creating a wide frequency spectrum of different types of traveling waves without disturbing the original setup.

To prove this concept experimentally an aluminum beam with a dimension of 1500mm × 25.4mm × 6.35mm (l×b×h) was selected for this experiment. Free-free boundary condition was used on this beam and shaker was attached at the $1/5^{th}$ of length of the beam. The shaker was attached to the beam using a stinger.

Few 3D printed fixtures were designed to hold the dashpot dampers while keeping them in contact with the beam. The damper 1, damper 2 and damper 3 were located at $4/5^{th}$, $3/5^{th}$ and $2/5^{th}$ the length of the beam respectively. The whole setup was attached to a shaker table. The piston rods of these dashpot dampers were glued to the beam.

Optomet's scanning laser vibrometer was used as a signal generator and a velocity measurement tool. The same procedure was followed to obtain the FRF of the system as mentioned in the chapter 2.

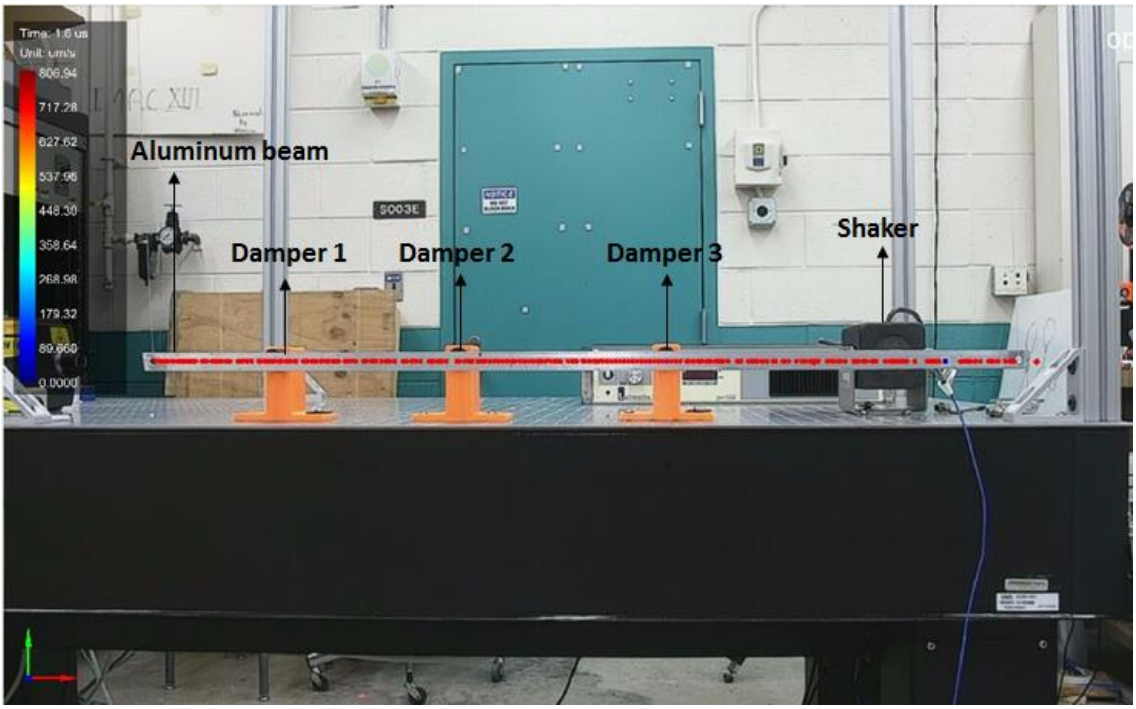

Figure 5.1: *Experimental setup for single point excitation method to generate TW*

This experiment resulted in successfully giving preliminary results for traveling wave generation at 4 different frequencies. The locations of traveling waves were depended on the location of the dashpot dampers. With these results it is proposed that, if further research is performed in this field, it would be having a lot of applications.

References

[1] Andrzej Sioma, Biologically Inspired Water Propulsion System, Journal of Bionic Engineering 10 (2013) 274-281

[2] Watts, Christopher Mark (2009) A comparison study of biologically inspired propulsion systems for an autonomous underwater vehicle. PhD thesis, University of Glasgow.

[3] V.V.N. Sriram Malladi, Mohammad Albarki, Patrick F. Musgrave and **Pablo A. Tarazaga,** Investigation of propulsive characteristics due to traveling waves in continuous finite media. Proceedings Volume 10162, Bio inspiration, biomimetics and bio replication (2017)

[4] Vijaya V.N. Sriram Malladi, Continual Traveling waves in finite structures: Theory Simulation, and Experimentation. 2016

[5] Patrick F. Musgrave, Turbulent Boundary Layer over a Piezoelectrically Excited Traveling wave surface. 2018

[6] Isil Anakok, A Study on Steady State Traveling Waves in Strings and Rods. 2018

[7] Ersan Demirer and **Yu-Cheng Wang,** Effect of actuation method on Hydrodynamics of Elastic Plates Oscillating at Resonance, J. Fluid Mech. (2021), Vol. 910, A4

[8] F.J. Fahy, Foundations of engineering acoustics, Academic press,2000

[9] R. R. Craig and **A.J. Kurdila,** Fundamentals of structural dynamics, John Wiley and Sons, 2006

[10] Machin K., Wave propagation along flagella, J. exp. Biol, Vol. 35, No. 4, pp. 796–806, 1958.

[11] Taylor G., Analysis of the swimming of microscopic organisms, Proceedings of the Royal Society of London A: Mathematical, Physical and Engineering Sciences, Vol. 209, pp. 447– 461, The Royal Society, 1951.

[12] M.A. Sleigh, Mechanisms of flagellar propulsion, Vol. 164, No. 1-3, pp. 45-53.

[13] Yonghua ZHANG, Shangrong LI and **Ji MA,** Development of an underwater Oscillatory propulsion system using shape memory alloy, Proceedings of IEEE, International conference on mechatronics & automation 2015.

[14] Joseph Najem, Stephen A Sarles, Biomimetic jellyfish-inspired underwater vehicle actuated by ionic polymer metal composite actuators. Smart Materials and Structures 21(9) September 2012

[15] Joel Hubbard, Maxwell Fleming, D.Pugal, Monolithic IPMC Fins for Propulsion and Maneuvering in Bio inspired Underwater Robotics. IEEE Journal of Oceanic Engineering July 2014

[16] Zhihang Ye, Piqi Hou, Zheng Chen, 2D maneuverable robotic fish propelled by multiple ionic polymer-metal composite artificial fins. International Journal of intelligent robotics and applications 1(2): 1-14 June 2017

[17] Patric F. Musgrave, Electro-hydro-elastic Modeling of Structure-Borne Traveling Waves and their application to aquatic swimming motions, Journal of Fluids and Structures 102 (2021) 103230

[18] Patrick F Musgrave, Mohammad I Albakri and **Austin A. Phoenix,** Guidelines and procedure for tailoring high-performance, steady state traveling waves for propulsion and solid-state motion, Smart Mater, Struc. 30 (2021) 025013 (14pp)

[19] Sodano H. A., Inman D. J. and **Park G.,** A review of power harvesting from vibration using piezoelectric materials, Shock and Vibration Digest, Vol. 36, No. 3, pp. 197–206, 2004.

[20] S.O.R. Moheimani, A survey of recent innovations in vibration damping and control using shunted piezoelectric transducers, IEEE Transactions on Control Systems Technology, Volume: 11 Issue:4

[21] Patrick F. Musgrave, Mohammad I. Albakri, Charles Tenney, Pablo A. Tarazaga, Generating and tailoring structure-Borne Traveling waves on two-dimensional surfaces, Journal of Sound and Vibration. Volume 480, August 2020, 115417

[22] S Motaharibidgoli, VVNS Malladi, PA Tarazaga, Generating Anechoic Traveling Wave in Beam with Various Boundary Conditions. Sensors and Instrumentation, Aircraft/Aerospace, energy Harvesting & dynamic Environment testing, Volume 7, Springer 2020

[23] VVNS Malladi, M Albakri, PA Tarazaga, An experimental and theoretical study of two-dimensional traveling waves in plates. Journal of Intelligent materials systems and structures 28 (13), 1803-1815

[24] Peter Avitabile, Modal testing: A Practitioner's Guide, 2018 John Wiley & Sons

[25] VVNS Malladi, D Avirovik, S Priya, PA Tarazaga, Travelling wave phenomenon through a piezoelectric actuation on a free-free beam. Smart Materials, Adaptive structures and intelligent systems 46148

[26] Patrick F Musgrave1, Mohammad I Albakri and Austin A Phoenix, Guidelines and procedure for tailoring high-performance, steady state traveling waves for propulsion and solid-state motion. Smart Materials and Structures Smart Mater. Struct. 30 (2021) 025013 (14pp) 15 June 2020

[27] https://cdn.stereolabs.com/assets/datasheets/zed2-camera-datasheet.pdf

[28] Zhang, Z., A Flexible New Technique for Camera Calibration. IEEE Transactions on Pattern Analysis and Machine Intelligence. Vol. 22, Number. 11, 2000, pp. 1330–1334.